1-1-1961

Transfer function of UTR-10 reactor using reactor oscillator technique

Paul Herbert Lustig
Iowa State University

TRANSFER FUNCTION OF UTR-10 REACTOR USING REACTOR OSCILLATOR TECHNIQUE

by

Paul Herbert Lustig

A Thesis Submitted to the
Graduate Faculty in Partial Fulfillment of
The Requirements for the Degree of
MASTER OF SCIENCE

Major Subject: Nuclear Engineering

Iowa State University
Of Science and Technology
Ames, Iowa

1961

TABLE OF CONTENTS

I. INTRODUCTION

The study of reactor kinetics has been growing over the past few years as swiftly as the new ideas in reactor concepts. Safety is equally as important a factor as power cost in the future development of feasible reactor power. Advanced reactor proposals must be analyzed kinetically to understand the limits to the stability of the reactor.

A useful device in analyzing a reactor system for its kinetic behavior is the so-called transfer function. The transfer function can be defined as the vector that represents the ratio of the output to the input of a system. This means that the transfer function specifies not only the magnitude of this ratio but also the phase relations between output and input. In existing reactors this phase and amplitude response is usually and conveniently measured by means of a sinusoidal input function. In electrical systems it might be a sinusoidal voltage impression while in chemical systems it may be sinusoidal variation in reactant concentration. Reactor systems may be conveniently investigated with sinusoidal variation in reactivity. The mathematical grounds for the determination of this frequency response is that if the phase and amplitude relations of a system are known for all input frequencies from zero to infinity or for practical purposes over all relevant ranges of frequencies then the response may be predicted for any type of input sinusoidal or transient. The transfer function is the manifestation of the frequency response: it is what can be used to predict the system response to any type of input.

The reactor transfer function of interest for the present is the

open loop transfer function. This means that there are no feedback effects (temperature changes in the fuel or moderator, control system rod adjustment, etc.) to affect the natural response of the reactor to the input. Servomechanism analysis can then be applied considering feedback systems to determine the overall behavior of the reactor system under any operating conditions.

The transfer function is arrived at through the time dependent differential equation that describes the change in the variable that is affected by the changing input in terms of that input. In other words for a reactor system a differential equation that shows the change in neutron population as a function of reactivity is desired. This latter is the reactor kinetic equation.

A. Development of Reactor Kinetic Equations and Transfer Function for Homogeneous Bare Core

In the formulation of the kinetic equations it is necessary to first develop a differential equation for the rate of change of neutron population with time, which naturally follows from a neutron balance. The method used is that of J. F. Hill (9). However, a change in nomenclature has been made so that consistency is maintained within this work. Reference to the nomenclature, Chapter XI, may be necessary where the parameters are not defined in the text. The inputs to the system are from two sources namely, prompt and delayed neutrons. Denote a mean thermal prompt neutron lifetime by

$$\ell_o = \frac{1}{v \Sigma_a}$$

where v is a mean neutron velocity for thermal neutrons and Σ_a is the absorption cross-section for only thermal neutrons. The rate of production of prompt thermal neutrons is

$$k \Sigma_a vn(1-\beta)$$

or

$$\frac{kn}{\ell_o}(1-\beta).$$

The production rate of delayed neutrons is $\lambda_i C_i$ for the ith group or $\sum_1^6 \lambda_i C_i$ for all groups. The total production is the sum of the delayed and prompt production.

Neutrons are lost by capture or escape from the reactor. The rate of capture is $nv\Sigma_a$ or n/ℓ_o while if

$$\mathcal{L} = \frac{\text{neutrons escaping from the reactor}}{\text{neutrons absorbed in the reactor}}$$

then the rate of leakage or escape is $n\mathcal{L}/\ell_o$ and the total losses are $n(1+\mathcal{L})/\ell_o$.

The change of neutron population with time is the difference between production and loss, namely

$$\frac{dn}{dt} = \frac{kn}{\ell_o}(1-\beta) + \sum_1^6 \lambda_i C_i - \frac{n}{\ell_o}(1+\mathcal{L}) \qquad (1)$$

which gives on rearrangement

$$\frac{dn}{dt} = \frac{n}{\ell_o}\left[k(1-\beta) - (1+\mathcal{L})\right] + \sum_1^6 \lambda_i C_i . \qquad (1a)$$

Define $k = \frac{k_{eff} - 1}{k_{eff}}$ and $k_{eff} = k/(1+\mathcal{L})$ which on combination,

yield $(1 + \mathcal{L}) = k(1-\delta k)$. Substitution in Equation 1a gives

$$\frac{dn}{dt} = \frac{nk}{\ell_o}\left[(1-\beta) - (1-\delta k)\right] + \sum_1^6 \lambda_i c_i$$

or

$$\frac{dn}{dt} = \frac{nk}{\ell_o}(\delta k - \beta) + \sum_1^6 \lambda_i c_i .$$

ℓ_o was defined for an infinite reactor so let ℓ^* be defined as the mean prompt neutron lifetime for a finite reactor. In doing so ℓ_o should logically be reduced by the factor k_{eff}/k. Hence, $\ell^* = \ell_o k_{eff}/k$.

The final form of the kinetic equation is

$$\frac{dn}{dt} = \frac{n}{\ell^*} k_{eff}(\delta k - \beta) + \sum_1^6 \lambda_i c_i . \qquad (2)$$

A balance for the delayed neutrons from each of the i groups may simply be written as follows:

$$\frac{dc_i}{dt} = \frac{k_{eff} n}{\ell^*} - \lambda_i c_i \qquad (3)$$

where the first term on the right side of the equation is the production of the ith delayed neutron emmitter and the second term is the decay of this emitter.

The kinetic equations, (2 and 3), have now been established for a homogeneous bare reactor. The next step is to develop a transfer function for such a reactor and see how it would respond to a sinusoidal input of reactivity (δk). The response of the reactor is manifested by the variation in the neutron population. In this analysis the method of Shultz (12) is applied. In order to simplify the approach the equations are first linearized, that is let

$$n = n_o + \delta n \quad \text{and}$$

$$C_i = C_{io} + \delta C_i .$$

In doing this the values of n and C_i are allowed to vary only slightly from the steady state value of n_o and C_{io} respectively. The product of the two factors as it appears in Equation 2 would normally yield the non-linear product $n(t) \cdot k(t)$ which cannot be handled easily since both are functions of time. With the specification that both δn and δk are small their product may be neglected. The substitutions will be made after some slight rearrangement of the equations.

Equation 2 may be written

$$\frac{dn}{dt} = \frac{n}{\ell^*} k_{eff}\, \delta k - \frac{n}{\ell^*} k_{eff} \beta + \sum_1^6 \lambda_i C_i$$

in which the last two terms are replaceable by

$$-\sum_1^6 \frac{dC_i}{dt} = - \frac{n k_{eff} \beta}{\ell^*} + \sum_1^6 \lambda_i C_i$$

from Equation 3. This yields

$$\frac{dn}{dt} = \frac{\delta k\, k_{eff}\, n}{\ell^*} - \sum_1^6 \frac{dC_i}{dt} . \qquad (4)$$

The k_{eff} must be eliminated from the equation since it also varies with changing δk. This is accomplished by assuming that the reactor is originally in the just critical condition when the change δk is introduced and that since δk is small the value of k_{eff} does not change significantly from 1. Equation 4 may be rewritten as

$$\frac{dn}{dt} = \frac{\delta k\, n}{\ell^*} - \sum_1^6 \frac{dC_i}{dt} . \qquad (4a)$$

The substitution of $n = n_o + \delta n$ and $C_i = C_{io} + \delta C_i$ can now be effected.

$$\frac{d(n_o + n)}{dt} = \frac{\delta k(n_o + \delta n)}{\ell^*} - \sum_1^6 \frac{d(C_{io} + \delta C_i)}{dt} .$$

The derivatives of the constant terms (steady-state) are zero, hence

$$\frac{d\,\delta n}{dt} = \frac{\delta k n_o}{\ell^*} - \sum_1^6 \frac{d\,\delta C_i}{dt} . \qquad (5)$$

The product $\delta k\, \delta n/\ell^*$ has been omitted as negligible compared to the other terms. Substitution of these variables in the second kinetic equation (Equation 3) yields

$$\frac{d\,\delta C_i}{dt} = \frac{\beta_i n_o}{\ell^*} + \frac{\beta_i \delta n}{\ell^*} - \lambda_i C_{io} - \lambda_i \delta C_i .$$

But when the steady-state condition of this equation is considered, that is

$$\frac{\beta_i n_o}{\ell^*} - \lambda_i C_{io} = 0 ,$$

the equation becomes finally

$$\frac{d\,\delta C_i}{dt} = \frac{\beta_i \delta n}{\ell^*} - \lambda_i \delta C_i . \qquad (6)$$

The usual method of handling these equations involves the use of the Laplace transformation. Taking the Laplace of Equation 5 and 6 yields

$$s\,\delta n(s) - \frac{d\,\delta n(0)}{dt} = \frac{n_o}{\ell^*}\delta k(s) - s\sum_1^6 \delta C_i(s) - \sum_1^6 \frac{d\,\delta C_i(0)}{dt}$$

and

$$s\,\delta C_i(s) - \frac{d\,\delta C_i(0)}{dt} = \frac{\beta_i}{\ell^*}\,\delta n(s) - \lambda_i\,\delta C_i(s) .$$

If it is assumed that all variables have attained a steady state previous to the input $\delta k(s)$ then the derivatives at $t = 0$ are all zero and may be dropped leaving

$$s\,\delta n(s) = \frac{n_o}{\ell^*}\,\delta k(s) - s\sum_1^6 \delta C_i(s) \tag{7}$$

and

$$s\,\delta C_i(s) = \frac{\beta_i}{\ell^*}\,\delta n(s) - \lambda_i \delta C_i(s) . \tag{8}$$

From Equation 8

$$\delta C_i(s) = \frac{\beta_i\ \delta n(s)}{\ell^*\ [s + \lambda_i]}$$

Substitution of this value in Equation 7 yields on transposition

$$\delta n(s)\left[s\left\{1 + \sum_1^6 \frac{\beta_i}{\ell^*\ (s+\lambda_i)}\right\}\right] = \frac{n_o}{\ell^*}\,\delta k(s)$$

and finally the transfer function defined as output divided by input is

$$\frac{\delta n(s)}{\delta k(s)} = \frac{n_o}{\ell^*}\left[\frac{1}{s\left[1 + \sum_1^6 \frac{\beta_i}{\ell^*(s + \lambda_i)}\right]}\right] . \tag{9}$$

It should be stressed at this point that this transfer function has been derived for a bare homogeneous reactor in the just critical state. The input δk can be of any form but it must be very small compared to one and the flux distribution should not be distrubed greatly from that to which the wave equation applies. This not only limits the

magnitude of δk, but also its spatial distribution.

B. Development of Kinetic Equations for a Two Core Reactor System

The UTR-10, far from being a bare homogeneous reactor, is not only heterogeneous and reflected but also contains two separate cores which are mildly coupled to one another. Coupling means that neutrons which escape from one core and travel through the internal graphite reflector can eventually find their way into the second core. It has been found that such a system, while it does exhibit a single stable period for the reactor as a whole, when it deviates from criticality will not necessarily show a single transfer function such as derived in the previous section (3). The reason for this is that the power levels in the two cores may be different. This phenomenon is termed flux tilting. If the degree of this imbalance is known then it is possible to obtain a transfer functions, one for each core, for each type of input that is possible. In the case of a two-core reactor the excess reactivity of each core as well as the coupling between them may be subject to oscillation which would yield six separate transfer functions. The system can be reduced to a single transfer function only if the flux level is equal in the two cores. This is easily seen from the transfer function when it is developed for a two-core system. The type of input which will be developed and experimentally applied is the sinusoidal variation of the coupling coefficient only. The method of development of the kinetic equations is similar to that of Baldwin (3).

The time dependent diffusion approximation may be applied to each core separately which gives in core 1

$$D_1\nabla^2 \phi_1(r,t) - \Sigma_{a1}\phi_1(r,t) + S_1(r,t) = 1/v \frac{\partial \phi_1(r,t)}{\partial t} \quad (10)$$

while a similar equation holds for the second core.

The source term can be considered to be composed of three contributions; prompt neutrons that are moderated within the core itself, delayed neutrons that are moderated within the core, and that component which originates in the other slab. The cores are assumed to be identical in all ways except that the flux levels may be different.

The prompt thermal source for each core is a result of the slowing down of prompt neutrons emitted in thermal fission (S_p). In core one this would be

$$S_p = (1-\beta)k_1 \Sigma_{a1} \mathcal{L}_1 \phi_1(r,t).$$

The delayed source (S_d) depends on the decay constants of each group and the concentration of each delayed neutron precursor. To consider only thermal neutrons this has to be multiplied by factors to correct for leakage and resonance absorption.

$$S_d = p_1 \mathcal{L}_1 \sum_1^6 \lambda_i c_{i1}(r,t) .$$

The final source term (S_{12}) coming from the second core is delayed by time τ in crossing the internal reflector. It is assumed proportional to the average flux in the other core hence

$$S_{12} = \epsilon_1 \bar{\phi}_2(t-\tau) .$$

The total thermal neutron source in the core 1 is the sum of these three terms

$$S_1 = S_p + S_d + S_{12} .$$

Substituting this source term in Equation 10, the diffusion equation, yields

$$D_1 \nabla^2 \phi_1(r,t) - \Sigma_{a1} \phi_1(r,t) + (1-\beta) k_1 \Sigma_{a1} \mathcal{L}_1 \phi_1(r,t)$$

$$+ p_1 \mathcal{L}_1 \sum_1^6 \lambda_i C_i(r,t) + \epsilon_1 \bar{\Phi}_2(t-\tau) = \frac{1}{v} \frac{\partial \phi_1(r,t)}{\partial t} . \quad (11)$$

The derivation of the kinetic equations and transfer function will be demonstrated only for core one.

The precursor equation, 3, naturally holds for each core.

$$\frac{\partial C_{i1}(r,t)}{\partial t} = - \lambda_i C_i(r.t) + \frac{k_1}{p_1} \beta_i \Sigma_{a1} \phi_1(r,t). \quad (12)$$

The assumption is made that the wave equation holds in each core which implies the separability of the variables r and t. Thus $- B^2 \phi_1(r,t) = \nabla^2 \phi_1(r,t)$. Make this substitution in Equation 11, divide by Σ_{a1} and set $D/\Sigma_{a1} = L_1^2$, the square of the thermal diffusion length. The following equation is obtained:

$$\phi_1(r,t) \left[- (L_1^2 B_1^2 + 1) + (1-\beta) k_1 \mathcal{L}_1 + \frac{p_1 \mathcal{L}_1}{\Sigma_{a1}} \sum_1^6 \frac{\lambda_i C_{i1}(r,t)}{\phi_1(r,t)} \right]$$

$$+ \frac{\epsilon_1 \bar{\Phi}_2(t-\tau)}{\Sigma_{a1}} = \frac{1}{v \Sigma_{a1}} \frac{\partial \phi_1(r.t)}{\partial t} . \quad (13)$$

But

$$\phi_1(r,t) = n_1(r,t)\, v; \quad l = 1/ v \Sigma_{a1}(1 + L_1^2 B_1^2); \quad k_1^{eff} = \frac{k_1 \mathcal{L}_1}{(1 + L_1^2 B_1^2)}$$

and set $\alpha_1 = \epsilon_1 / \Sigma_{a1}(1 + L_1^2 B_1^2)$. The assumption that ϕ_2 can be represented as an average flux in the source term is valid for small highly reflected cores such as in the UTR-10 reactor. Equation 13 becomes

$$n_1(r,t)v \left[-1 + (1-\beta)k_1^{eff} + \frac{p_1 \mathcal{L}_1 \ell_1}{n_1(r,t)} \sum_1^6 \lambda_i c_{i1}(r,t) \right]$$

$$+ \alpha_1 n_2(t-\tau)v = \ell_1 v \frac{\partial n_1(r,t)}{\partial t} . \qquad (14)$$

From the precursor equations substitute for $\lambda_i c_i(r,t)$ in Equation 14, that is from Equation 12

$$\sum_1^6 \lambda_i c_i(r,t) = \sum_1^6 \frac{k_1 \beta_i}{p_1} \Sigma_{a1} v n_1(r,t) - \sum_1^6 \frac{\partial c_i(r,t)}{\partial t}$$

or with the substitutions above this expression becomes

$$\sum_1^6 \lambda_i c_i(r,t) = \sum_1^6 \frac{k_1^{eff} \beta_i}{p_1 \mathcal{L}_1 \ell_1} n_1(r,t) - \sum_1^6 \frac{\partial c_{i1}(r,t)}{\partial t} . \qquad (15)$$

This gives upon substitution in Equation 14

$$n_1(r,t)v \left[-1 + (1-\beta)k_1^{eff} + k_1^{eff} \sum_1^6 \beta_i - \right.$$

$$\left. \frac{p_1 \mathcal{L}_1 \ell_1}{n_1(r,t)} \sum_1^6 \frac{\partial c_i(r,t)}{\partial t} \right] + \alpha_1 n_2(t-\tau)v = \ell_1 v \frac{\partial n_1(r,t)}{\partial t} . \qquad (16)$$

With $\sum_{1}^{6} \beta_i = \beta$ and $k_1^{eff} - 1 = k_1^{ex}$ Equation 16 becomes

$$\frac{k_1^{ex}}{\ell_1} n_1(t) - p_1 \mathcal{L}_1 \sum_{1}^{6} \frac{\partial c_{i1}(t)}{\partial t} + \frac{\alpha_1 n_2(t-\tau)}{\ell_1} = \frac{\partial n_1(t)}{\partial t} . \quad (17)$$

The functional dependence of n on position has been dropped in accordance with the separability of the variables previously implied.

The precursor equation is from Equation 15,

$$\frac{\partial c_{i1}(t)}{\partial t} = -\lambda_i c_{i1}(t) + \frac{k_1^{eff} \beta_i}{p_1 \mathcal{L}_1 \ell_1} n_1(t). \quad (18)$$

Equation 17 and 18 are the kinetic equations which will now be used to derive the two-core transfer function by the method of Laplace transformations. Similar equations apply to core 2. Again, however, the equations will only be derived for the one core.

Assume an input of the form

$$\alpha_1 = \alpha_2 = \alpha_o + \delta\alpha .$$

The form of the output variables will be

$$n_1 = n_1^{\circ} + \delta n_1$$

$$c_{i1} = c_{i1}^{\circ} + \delta c_{i1} .$$

Substituting these in the kinetic equations the following is obtained:

$$\frac{k_1^{ex} n_1^{\circ}}{\ell_1} + \frac{k_1^{ex} \delta n_1(t)}{\ell_1} - p_1 \mathcal{L}_1 \sum_{1}^{6} \frac{\partial \delta c_{i1}(t)}{\partial t} + \frac{\alpha_o n_2^{\circ}(t-\tau)}{\ell_1}$$

$$\frac{\alpha_o \delta n_2(t-\tau)}{\ell_1} + \frac{\delta\alpha n_2^{\circ}(t-\tau)}{\ell_1} + \frac{\delta\alpha \delta n_2(t-\tau)}{\ell_1} = \frac{\partial n_1(t)}{\partial t} . \quad (19)$$

The term $\frac{\delta\alpha\ \delta n(t-\tau)}{\ell_1}$ may be neglected and from the steady-state condition, $\frac{k_1^{ex} n_1^o}{\ell_1} + \frac{\alpha_o n_2^o}{\ell_1} = 0$, the Equation 19 reduces to

$$\frac{k_1^{ex}\delta n_1(t)}{\ell_1} - p_1 \mathcal{L}_1 \sum_1^6 \frac{\partial \delta c_{i1}(t)}{\partial t} + \frac{\alpha_o\, \delta n_2(t-\tau)}{\ell_1}$$

$$+ \frac{\delta\alpha\ n_2^o(t-\tau)}{\ell_1} = \frac{\partial n_1(t)}{\partial t}. \qquad (20)$$

Substitute the output variables as defined above in the precursor equation (18) and as in the case of the diffusion equation the steady state condition can be dropped, that is

$$- \lambda_i c_{i1}^o + \frac{k_1^{eff} n_1^o \beta_i}{p_1 \mathcal{L}_1 \ell_1} = 0.$$

The resulting equation is

$$\frac{d\,\delta c_{i1}(t)}{dt} = - \lambda_i\, \delta c_{i1}(t) + \frac{k_1^{eff} \beta_i\, \delta n_1(t)}{p_1 \mathcal{L}_1 \ell_1}. \qquad (21)$$

Take the Laplace transform of the two equations (20 and 21).

$$\frac{k_1^{ex}}{\ell_1} \delta n_1(s) - p_1 \mathcal{L}_1 \sum_1^6 s c_{i1}(s) + \frac{\alpha_o}{\ell_1} \delta n_2(s) e^{-s\tau}$$

$$+ \frac{\delta\alpha(s) n_2^o}{\ell_1} = s\, \delta n_1(s). \qquad (22)$$

$$s\, \delta c_{i1}(s) = - \lambda_i c_{i1}(s) + \frac{k_1^{eff} \beta_i \delta n_1(s)}{p_1 \mathcal{L}_1 \ell_1}. \qquad (23)$$

Solve for $\delta C_{i1}(s)$ in Equation 23.

$$\delta C_{i1}(s) = \frac{k_1^{eff} \beta_i \delta n_1(s)}{P_1 \ell_1 \ell_1 (s + \lambda_i)} .$$

Substitution of this in Equation 22 yields

$$\frac{k_1^{ex}}{\ell_1} \delta n_1(s) - \sum_1^6 \frac{k_1^{eff} \beta_i s \delta n_1(s)}{\ell_1 (s + \lambda_i)} + \frac{\alpha_o \delta n_2(s) e^{-s\tau}}{\ell_1}$$

$$+ \frac{\delta \alpha(s) n_2^o}{\ell_1} = s \delta n_1(s) .$$

Rearranging these equations to see the coefficients of δn_1 and δn_2 the following is found:

$$\left[\frac{k_1^{ex}}{\ell_1} - \sum_1^6 \frac{k_1^{eff} \beta_i}{\ell_1} \frac{s}{(s + \lambda_i)} - s \right] \delta n_1(s) + \frac{\alpha_o e^{-s\tau} \delta n_2(s)}{\ell_1}$$

$$= - \frac{\delta \alpha(s) n_2^o}{\ell_1} . \qquad (24)$$

In the critical system with α at its median value α_o kinetic Equation 17 yields

$$k_1^{ex} n_1^o + \alpha_o n_2^o = 0 .$$

Hence it is seen that R defined as n_1^o/n_2^o is also equal to $- \alpha_o / k_1^{ex}$. Substitution of $R = n_1^o/n_2^o$, $\alpha_o = - R k_1^{ex}$ and $k_1^{eff} = 1 + k^{ex}$ into Equation 24 gives

$$\left[- \frac{\alpha_o}{R \ell_1} - \frac{(1 - \alpha_o/R)}{\ell_1} \sum_1^6 \frac{\beta_i s}{s + \lambda_i} - s \right] \delta n_1(s) + \frac{\alpha_o e^{-s\tau} \delta n_2(s)}{\ell_1}$$

$$= - \frac{\delta \alpha(s) n_2^o}{\ell_1} .$$

Multiply this equation by $-\ell_1 R / \delta\alpha(s) n_1^{\circ}$.

$$\left[\alpha_o + (R - \alpha_o) \sum_1^6 \frac{\beta_i s}{(s + \lambda_i)} + sR\ell_1\right] \frac{\delta n_1(s)}{\delta\alpha(s) n_1^{\circ}}$$

$$- \alpha_o e^{-s\tau} \frac{\delta n_2(s)}{\delta\alpha(s) n_2^{\circ}} = 1 .$$

Through a similar manipulation of the diffusion equation for the second core, the equation in terms of the transfer function variables is

$$- \frac{\alpha_o e^{-s\tau} \delta n_1(s)}{\delta\alpha(s)\, n_1^{\circ}} + \left[\alpha_o + (1/R - \alpha_o) \sum_1^6 \frac{\beta_i s}{(s + \lambda_i)}\right.$$

$$\left. + \frac{s\ell_2}{R}\right] \frac{\delta n_2(s)}{\delta\alpha(s) n_2^{\circ}} = 1 .$$

These simultaneous equations in the transfer function variables for the two cores, that is $\frac{\delta n_1(s)}{\delta\alpha(s) n_1^{\circ}}$ and $\frac{\delta n_2(s)}{\delta\alpha(s) n_2^{\circ}}$, can be solved by determinants or simply algebraically. The results are as follows:

$$\frac{\delta n_1(s)}{\delta\alpha(s) n_1^{\circ}} =$$

$$\frac{\left[\alpha_o + (1/R - \alpha_o) \sum_1^6 \frac{\beta_i s}{(s + \lambda_i)} + \frac{s\ell_2}{R}\right] + \alpha_o e^{-s\tau}}{\left[\alpha_o + (1/R - \alpha_o) \sum_1^6 \frac{\beta_i s}{(s + \lambda_i)} + \frac{s\ell_2}{R}\right] \left[\alpha_o + (R - \alpha_o) \sum_1^6 \frac{\beta_i s}{(s + \lambda_i)} + s\ell_1 R\right] - \alpha_o^2 e^{-2s\tau}}$$

and

$$\frac{\delta n_2(s)}{\delta \alpha(s) n_2^{\circ}} =$$

$$\frac{\left[\alpha_o + (R - \alpha_o)\sum_1^6 \frac{\beta_i s}{(s+\lambda_i)} + s\ell_1 R\right] + \alpha_o e^{-s\tau}}{\left[\alpha_o + (1/R - \alpha_o)\sum_1^6 \frac{\beta_i s}{(s+\lambda_i)} + \frac{s\ell_2}{R}\right]\left[\alpha_o + (R-\alpha_o)\sum_1^6 \frac{\beta_i s}{(s+\lambda_i)} + s\ell_1 R\right] - \alpha_o^2 e^{-2s\tau}}.$$

As is easily seen the transfer functions are identical only for $R = 1$, that is when the flux levels in the two cores are equal.

In this study an attempt was made to determine the value of the mean prompt thermal neutron lifetime, ℓ. It was known that if the two core response was similar to single core response the value may be arrived at through the break frequency which occurs at $\beta/\ell + \lambda$ (see Equation 9) or approximately β/ℓ. To see this let $\sum_1^6 \frac{\beta_i}{\ell(s+\lambda_i)}$ in Equation 9 reduce to $\frac{\beta}{\ell(s+\lambda)}$ where λ represents the averaged decay constant of all six groups. The transfer function then reduced to

$$\frac{\delta n(s)}{\delta k(s)} = \frac{n_o}{\ell^*}\left[\frac{s+\lambda}{s(s+\frac{\beta}{\ell}+\lambda)}\right].$$

The break frequency of interest is in the denominator. Neglection of λ and assumption of β would yield the desired value of ℓ once the experimental break frequency were known. However, it was thought necessary to investigate and analyze the two-core transfer function derived above to see if it did correspond to the single core function. The method and results of this research are presented in the following chapter.

II. ANALYSIS OF TWO CORE TRANSFER FUNCTION

It is not readily obvious what the two-core transfer function is like and whether or not it is comparable to the single core transfer function previously derived. In order to place it in a form where the two may be compared first assume a single group of delayed neutrons with average properties of all six groups. The transfer function for the first core reduces to

$$T.F._1 = \frac{\left[\alpha_o + (1/R - \alpha_o)\frac{\beta s}{s+\lambda} + \frac{s\ell_1}{R}\right] + \alpha_o e^{-s\tau}}{\left[\alpha_o + (1/R - \alpha_o)\frac{\beta s}{s+\lambda} + \frac{s\ell_1}{R}\right]\left[\alpha_o + (R - \alpha_o)\frac{\beta s}{s+\lambda} + s\ell_1 R\right] - \alpha_o^2 e^{-2s\tau}} .$$

This expression may be most easily reduced to analyzable form by setting $R = 1$ and letting $\ell_1 = \ell_2 = \ell$. The factors of the right side of the denominator are then identical and the function becomes

$$T.F._1 = \frac{1}{\left[\alpha_o(1 - e^{-s\tau}) + (1 - \alpha_o)\frac{\beta s}{s+\lambda} + s\ell\right]} .$$

The factor $1 - e^{-s\tau}$ may be approximated by $s\tau$ and the function is

$$T.F._1 = \frac{s + \lambda}{s\ell\left[s + \frac{(1 - \alpha_o)}{(\alpha_o\tau/\ell + 1)}\frac{\beta}{\ell} + \lambda\right]} .$$

Physically in the UTR-10 this equation is approximately the same as the simple single core transfer function. τ and ℓ are the same order of magnitude and $\alpha_o \ll 1$. This function when plotted on a Bode

amplitude diagram which is standard procedure in transfer function analysis has the following characteristics:

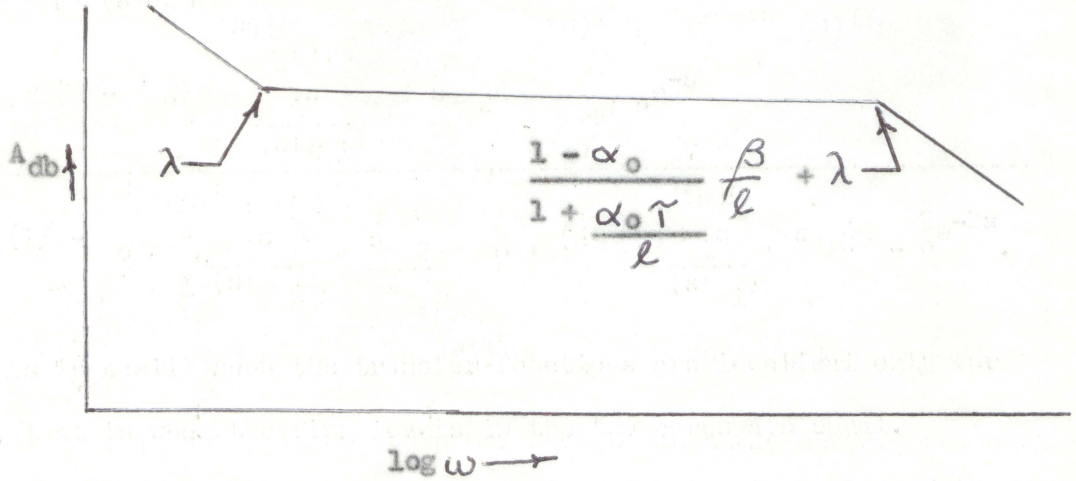

In this and subsequent diagrams in the discussion the amplitude curve is approximated by its asymptotes.

The corner frequencies of this curve occur at λ and $\frac{\beta}{\ell} + \lambda$ or more precisely for the two core function with R = 1 at λ and at

$$\frac{(1-\alpha_o)}{(1+\frac{\alpha_o \tau}{\ell})} \frac{\beta}{\ell} + \lambda .$$

As was mentioned previously, for the two core system, the flux levels in the slabs need not and probably will not be the same. For this reason the transfer function as a function of R as well as the other parameters are subject to investigation. The assumption $\ell_1 = \ell_2 = \ell$ is still maintained. In order to obtain the essential information such as break frequency without resorting to the use of numerical values for the parameters, it was found useful to investigate the high and low frequency response separately. Of course it is

necessary to know the approximate magnitudes of these quantities before it can be said which terms may be neglected. For this purpose the values used by Danofsky (5) were adapted.

Consider first very low frequencies. The transfer function for the first core becomes

$$T.F._1 = \frac{\left[\alpha_o + (1/R - \alpha_o)\frac{\beta s}{s+\lambda} + \alpha_o\right]}{\left[\alpha_o + (1/R - \alpha_o)\frac{\beta s}{s+\lambda}\right]\left[\alpha_o + (R - \alpha_o)\frac{\beta s}{s+\lambda}\right] - \alpha_o^2}.$$

Here the terms $s\,\ell/R$ and $s\,\ell R$ have been neglected and the terms $e^{-s\tau}$ and $e^{-2s\tau}$ have been set equal to unity. In all these cases the Laplacian operator, s, has been assigned the value of the frequency. A further simplification that may be made is that of neglecting α_o with respect to both R and 1/R. This is not necessary in the analysis but was simply done for convenience. If it is desired, in the result, R and 1/R may be replaced by $(R - \alpha_o)$ and $(1/R - \alpha_o)$ respectively. With the expansion of the terms in the denominator and placement of all terms over the common denominator $(s + \lambda)$ the transfer function becomes

$$T.F._1 \quad \frac{\left[(2R\alpha_o + \beta)s + 2R\alpha_o\lambda\right]\quad(s+\lambda)}{s\quad\left[\alpha_o\beta(1/R + R + \beta/\alpha_o)s + \quad \lambda\alpha_o\beta(1/R + R)\right]}.$$

This may be placed in a form where the break frequencies are represented by the constant terms in each factor as does λ in $(s + \lambda)$. Thus

$$T.F._1 = \frac{\left[s + \frac{2R\,\alpha_o\,\lambda}{2R\,\alpha_o + \beta}\right](s + \lambda)}{s\left[s + \frac{(R + 1/R)\,\lambda}{(R + 1/R + \frac{\beta}{\alpha_o})}\right]} .$$

The gain factor has been disregarded.

The magnitudes suggested by Danofsky (5) for the parameters were*

$\beta = 0.0065$

$\lambda = 0.08$ disintegrations/sec.

$\tau = 2.1 \times 10^{-4}$ sec.

$\ell = 1.35 \times 10^{-4}$ sec.

$\alpha_o = 0.0155$

$R = 1.2$.

The use of these values in the above transfer function yields

$$T.F._1 = \frac{(s + 0.068)(s + 0.08)}{s(s + 0.066)} .$$

This will appear as follows on a Bode amplitude plot which shows the asymptotic transfer function:

---

*The value of τ was calculated by Danofsky. λ was simply a weighted average decay constant for the six groups of delayed neutrons. R was assumed applicable to UTR-10 operation by Danofsky. The value of ℓ was given by the American Standard Company (14) while α_o was estimated by Ray F. Crews, Manager of Applications Engineering-Nuclear, American Standard Company, Mountain View, California, Information concerning the UTR-10 reactor, private communication, 1959. β was that given by Keppin and Wimett (10a).

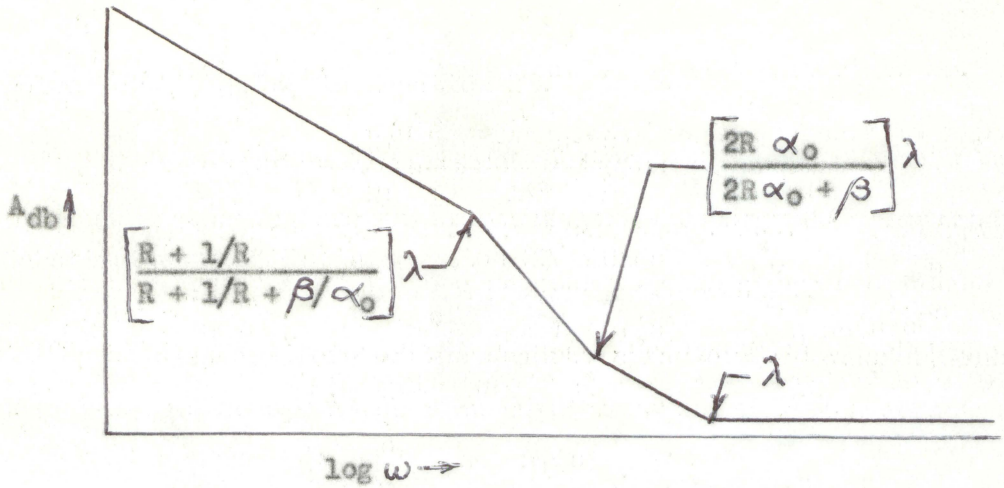

This transfer function is valid for the low frequencies suggested by the values obtained for the break frequencies and lower as well as up to the order of magnitude of one radian per second. It can be seen that the break at 0.08 or λ still occurs as in the single core function but there is a short interval preceding this where the slope changes to -12 db/octave and then quickly shifts back to -6 db/octave.

Consider the transfer function at high frequencies above 10 radians per second. In this case the term $s/(s + \lambda)$ may be considered as unity whereupon the transfer function is

$$T.F._1 = \frac{\left[\alpha_o + \frac{\beta}{R} + \frac{s\ell}{R}\right] + \alpha_o(1 - s\tau)}{\alpha_o^2 + \alpha_o\beta R + \alpha_o \ell R s + \beta^2 + \frac{\alpha_o\beta}{R} + 2\beta\ell s + \frac{\alpha_o \ell s}{R} + \ell^2 s^2 - \alpha_o^2(1-s\tau)}.$$

In this case $e^{-s\tau}$ was approximated by $1-s\tau$ and similarly $e^{-2s\tau}$ by $1-2s\tau$. The terms in the denominator can be combined into a quadratic term and the function becomes

$$T.F._1 = \frac{\left[2\alpha_o + \frac{\beta}{R}\right] + \left[\frac{\ell}{R} - \alpha_o\tau\right] s}{\left[\alpha_o\beta R + \beta^2 + \frac{\alpha_o\beta}{R}\right] + \left[\alpha_o\ell R + 2\beta\ell + \frac{\alpha_o\ell}{R} + 2\alpha_o^2\tau\right] s + \ell^2 s^2} .$$

The standard form of the quadratic factor in transfer function notation is

$$1 + \frac{2\zeta}{\omega} s + \frac{s^2}{\omega^2}$$

so that the function should be written as follows:

$$T.F._1 = \left[\frac{\frac{\ell}{R} - \alpha_o\tau}{\alpha_o\beta_b}\right]\left[\frac{2\alpha_o + \frac{\beta}{R}}{\frac{\ell}{R} - \alpha_o\tau} + s\right] \Big/ \left[1 + \frac{\alpha_o a}{\sqrt{\alpha_o\beta_b}} \frac{s}{\sqrt{\frac{\alpha_o\beta_b}{\ell^2}}} + \frac{s^2}{\frac{\alpha_o\beta_b}{\ell^2}}\right]$$

where $a = R + 1/R + 2\beta/\alpha_o + 2\alpha_o\tau/\ell$

and $b = R + 1/R + \beta/\alpha_o$

ζ is then $= \frac{\alpha_o a}{2\sqrt{\alpha_o\beta_b}}$

and $\omega = \frac{\sqrt{\alpha_o\beta_b}}{\ell}$.

Whether or not this factor remains as a quadratic or can be factored into two linear functions depends on the value of ζ. If ζ is greater than or equal to unity then the function can and must be factored; if less than unity then it remains a quadratic and can be treated as such. If the magnitude of the parameters as stated previously are used then

the value of ζ is 1.46, however, it can be shown that independent of the values of the parameters ζ will always be greater than one. This means that the denominator must be reduced to two linear components. The roots of the quadratic represented by

$$\omega^2 + 2\zeta\omega s + s^2 = 0 \quad \text{are}$$

$$s = \omega\left[\zeta \pm \sqrt{\zeta^2 - 1}\right].$$

The use of these roots in the transfer function gives, again disregarding the gain factor

$$\text{T.F.}_1 = \frac{\left[\dfrac{2\alpha_o + \dfrac{\beta}{R} + s}{\dfrac{\ell}{R} - \alpha_o\tau}\right]}{\left[s + \dfrac{\alpha_o a + \sqrt{\alpha_o{}^2 a^2 - 4\alpha_o\beta_b}}{2\ell}\right]\left[s + \dfrac{\alpha_o a - \sqrt{\alpha_o{}^2 a^2 - 4\alpha_o\beta_b}}{2\ell}\right]}.$$

If the values recommended by Danofsky (5) are used the transfer function becomes

$$\text{T.F.}_1 = \frac{(347 + s)}{(288 + s)(46.8 + s)}.$$

This transfer function will appear as follows on the Bode amplitude diagram:

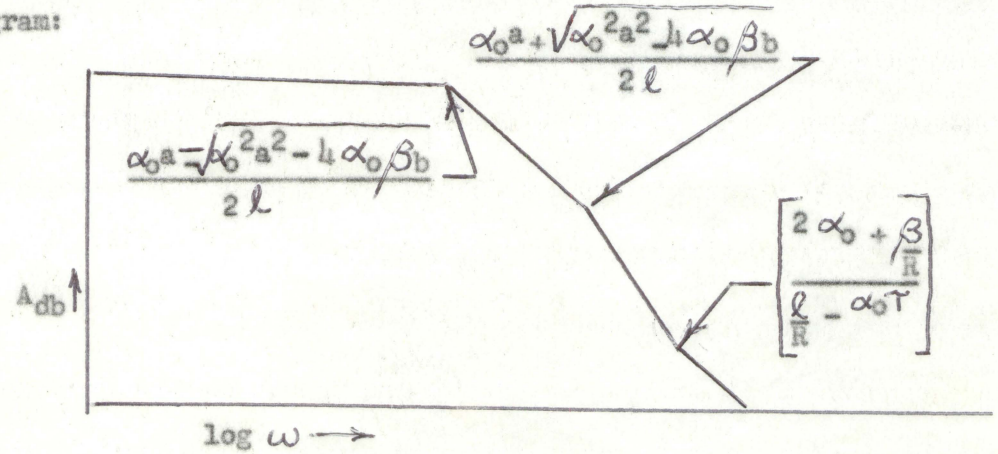

The complete transfer function for the two core system will be the combination of the low frequency response derived previously and the high frequency response above.

The subject of this study will be mainly the break that occurs at a frequency of approximately 46.8 radians per second as given by Danofsky's values. The remainder of this discussion will center on the properties of this break frequency and the parameters that determine it.

The transfer function for the high frequencies may be further reduced if we neglect the last term of the defined value of a, that is $2\alpha_0\tau/\ell$. Then $b = a + \beta/\alpha_0$. The transfer function reduces to;

$$T.F._1 = \frac{\left[\dfrac{2\alpha_0 + \dfrac{\beta}{R}}{\dfrac{\ell}{R} - \alpha_0\tau}\right] + s}{\left[s + \dfrac{\beta}{\ell}\right]\left[s + \dfrac{\alpha_0 a + \beta}{\ell}\right]} .$$

It is then in the frequency range of β/ℓ that a break should occur in the transfer function. This break and the one at λ are the ones that correspond the single core transfer function. If it is assumed that β is known for the reactor then ℓ may be determined once the experimental value of the break frequency is known. This is, however, an approximate analysis of the approximated high frequency response. In arriving at this transfer function λ was first neglected with respect to the frequency of oscillation. Further the term $\alpha_0\tau/\ell$ was neglected with respect to β/α_0. This is a valid assumption if α_0 is not much larger than that assumed by Danofsky (5), that is, 0.0155. The above transfer function can be applied with reasonable accuracy to the UTR-10 reactor with the degree of coupling

that exists. The break frequency that is obtained using the above approximation is 48.1 radians per second while the more precise first approximation gave a break frequency of 46.8 radians per second. There is a difference then of only 2.7% between the two approximations. It is also estimated that the neglect of λ in the original high frequency analysis will yield a 0.2% error at this frequency. This first approximation is then by far more accurate than the second. Of course the error will grow larger as α_o increases. Figure 1 shows the variation of the break frequency as α_o is varied maintaining all other parameters constant. It also compares this variation with the limiting frequency, as α_o approaches 0, of β/ℓ.

As can be seen from the graph the break frequency decreases rather slowly as α_o increases and the error introduced by neglecting α_o is not more than 5% for α_o less than .030 which is probably a valid assumption in the UTR-10. However so this may be valid the break frequency obtained experimentally was used to find the limiting value of ℓ from the β/ℓ approximation as well as ℓ as a function of α_o. To accomplish this the values of β, τ and R had to be assumed and throughout the values given by Danofsky (5) were utilized.

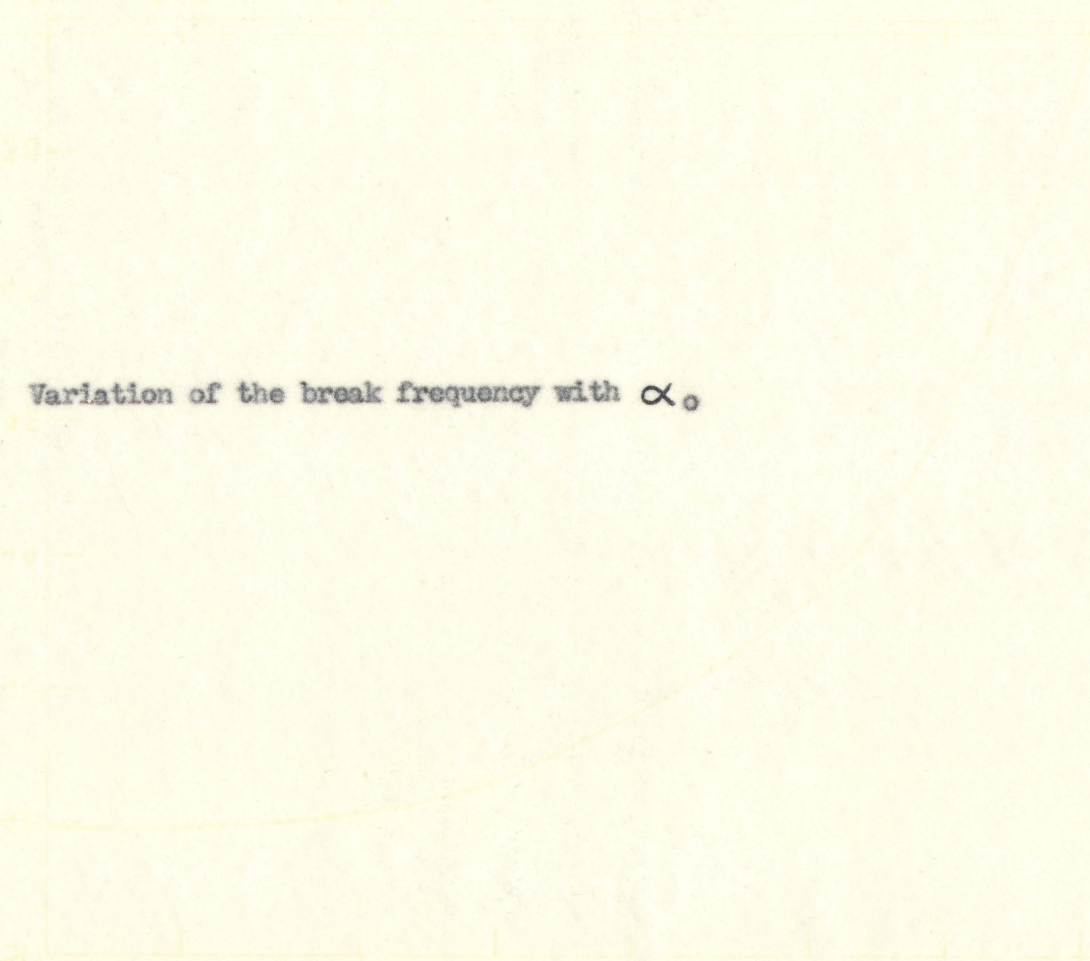

Figure 1. Variation of the break frequency with α_o

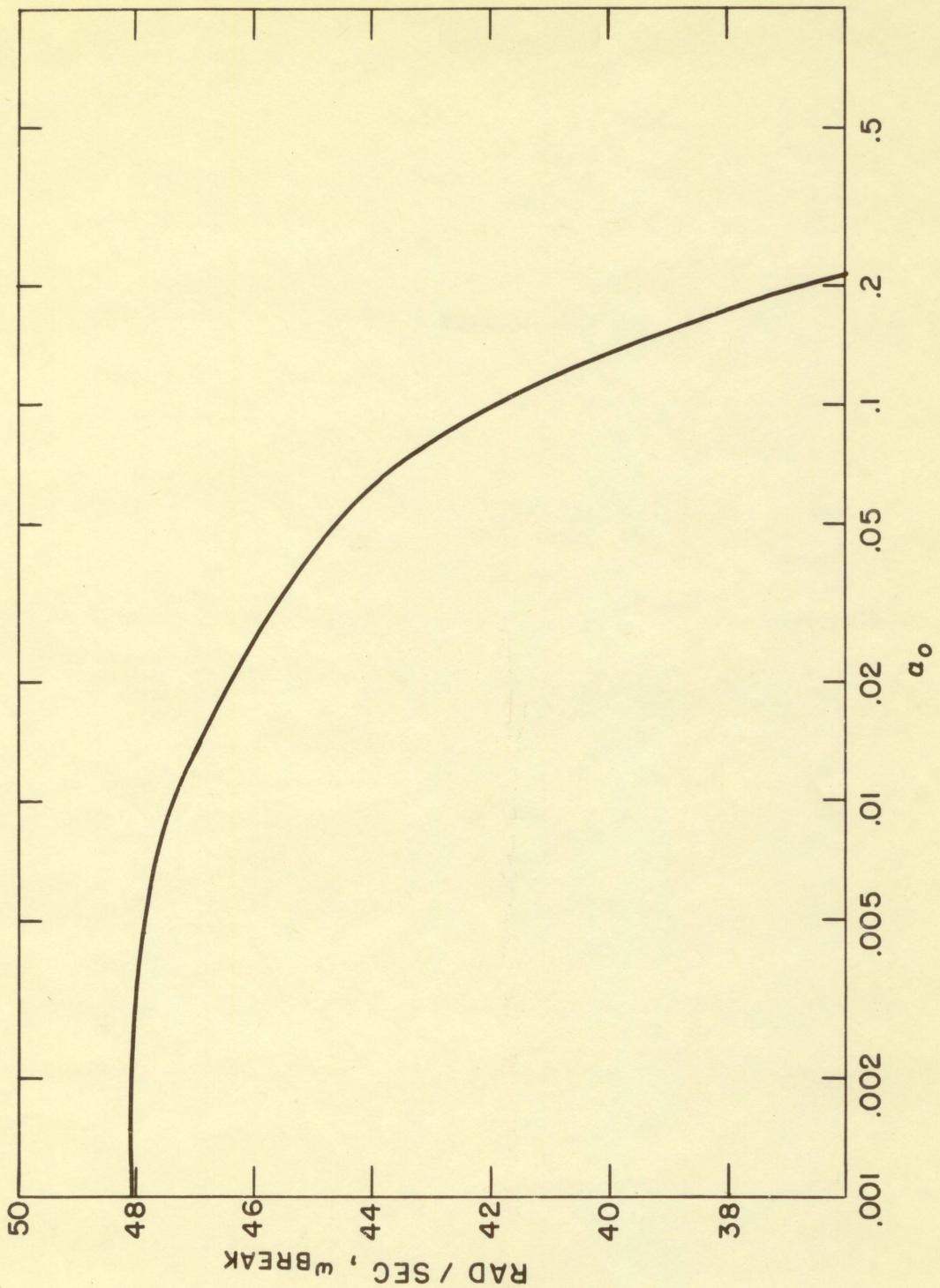
50
48
46
44
42
40
38
RAD / SEC , ω_{BREAK}
.001
.002
.005
.01
.02
.05
.1
.2
.5
a_o

III. REVIEW OF THE LITERATURE

The study of the kinetics of reactor systems was done on a theoretical basis with the first work on the Manhattan Project. Since then many have solved and resolved the kinetic equations using a variety of techniques for their different aims in applications (1, 6, 7, 9, 11, 12, 13). The foremost application is toward the better understanding of the reactor as a unit in a control system. Information along these lines is obtained through the transfer function. The reactor response to various reactivity changes will disclose the transfer function. This may be a step or ramp input, but as mentioned previously easiest to analyze is the sinusoidal input and response. This section discusses the various attempts at this latter technique along both theoretical and experimental lines.

Lundholm et al (10b) have investigated the SRE transfer function using frequency response techniques. They utilized both random noise analysis and reactor oscillation. The results of these two studies were each consistent with theory within experimental accuracy. The transfer function as derived for a single homogeneous core fit the experimental results obtained with respect to both phase relation and amplitude.

Much earlier work than this had been done to describe the transfer function of the CP-2 by Harrer et al (8). He used a cadmium oscillator located at the center of the CP-2. The results again agreed with the calculated simple transfer function. All of the data were taken above 0.2 radians per second oscillation frequency.

Similar work was done on KEWB by R. N. Cordy (4) using rows of

cadmium shades (rotor) and spots (stator) as the oscillation device. The number of rows determined the reactivity input amplitude. His results agreed well with the transfer function as derived for a water boiler reactor. This transfer function as opposed to the zero power transfer function previously derived in the introduction takes into account temperature and void effects. His data correspond to his derived transfer function but it is interesting to note that his results show a seventh group of delayed neutrons which he concludes arises from the delaying effect of the reflector in returning neutrons to the core.

Coupled reactors in general are considered by Avery (2). He considers the interaction of a system of cores each supplying neutrons to all the other cores. He then applies this theory to two coupled reactors. Perturbation theory is used to obtain reactivity as a function of a perturbed value of β which he defines through the importance function. He develops the inhour equation for a two core system.

Baldwin (3), as is shown in the introduction, uses two core kinetic equations to develop a transfer function which considers only sinusoidal variation of α_0, the coupling between cores, holding k^{ex} for each core at a constant value. This input is accomplished by placing a varying absorber in the center of the internal reflector. His derivation shows that if the flux level in the two cores differ then the transfer function for each core will be different.

Danofsky (5) used an analog circuit of the two core system represented by the UTR-10 reactor. After performing a variety of inputs on the electrical analog of this system he concluded that the response of the UTR-10 to a sinusoidal variation of the coupling with or without flux

tilting would not be significantly different than the response of a single region reactor under the same conditions of reactivity variation. During normal operation this flux tilting may vary from 1.05 to 1.18 which did not result in significant effects on the transfer function to make it very different from the single region reactor transfer function.

IV. THE EXPERIMENT

A. Equipment

Photographs of the three major components appear in Figures 2, 3 and 4. These are the oscillator units, the drive mechanism and the electronic equipment. Diagrams of the oscillator and pattern can be found in Figure 5.

The rotor with its half cylindrical pattern when rotated against the sinusoidal cadmium pattern of the stator gave an approximate sinusoidal reactivity variation. The actual variation is shown under results as Figure 6. The amplitude of variation was 0.0041. This arrangement gave one cycle per revolution so that at the maximum speed obtainable which was 1500 r.p.m. the oscillation frequency was 157 radians per second. This was well above the estimated 46.8 radians per second for the break frequency corresponding approximately to β/ℓ . The lowest frequency practically obtainable was .32 radians per second which corresponded to a speed of 3.1 r.p.m. which did not yield the transfer function in the range of the break at 0.08 radians per second predicted by the previous analysis.

The patterns were glued to both the stator and the rotor with thin steel wire stabilizing the rotor pattern. This was done as a safety precaution since the static worth of the cadmium was found to be approximately 0.25% which if added as a step input could produce a short period.

The position of the oscillating unit and the ion chamber as they were used in the reactor is shown in Figure 7.

The output of the reactor was detected by a compensated ion chamber

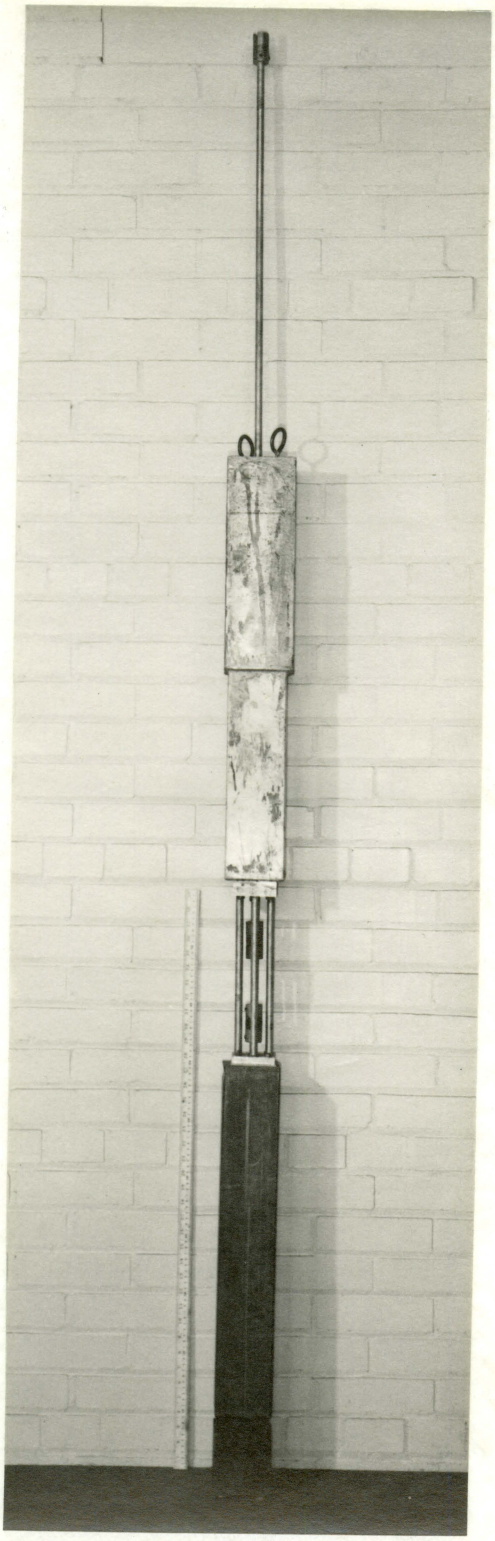

Figure 2. Oscillator unit

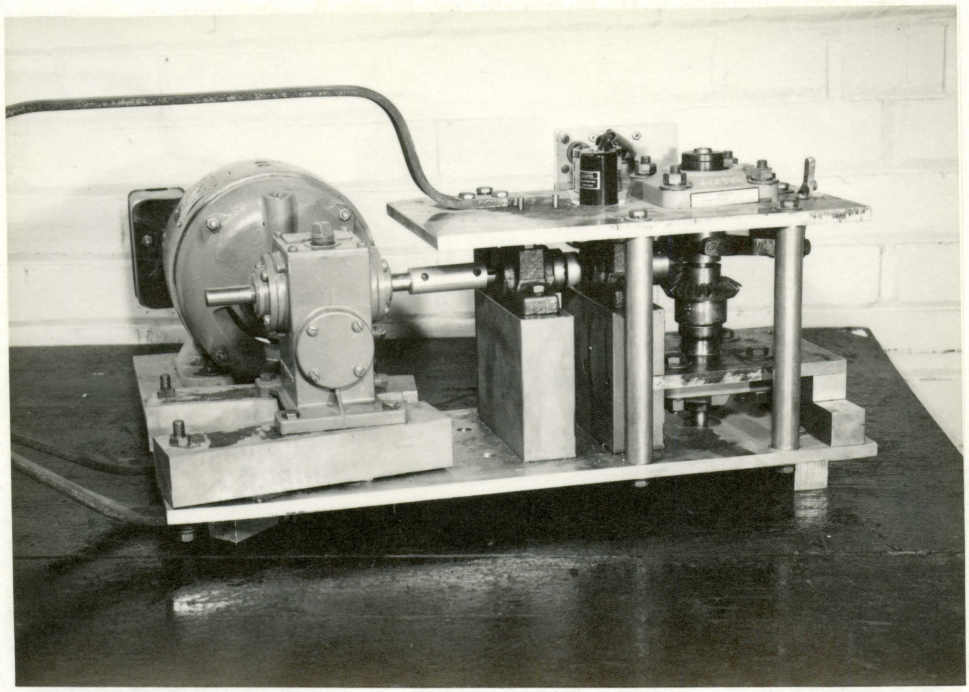

Figure 3. Drive mechanism

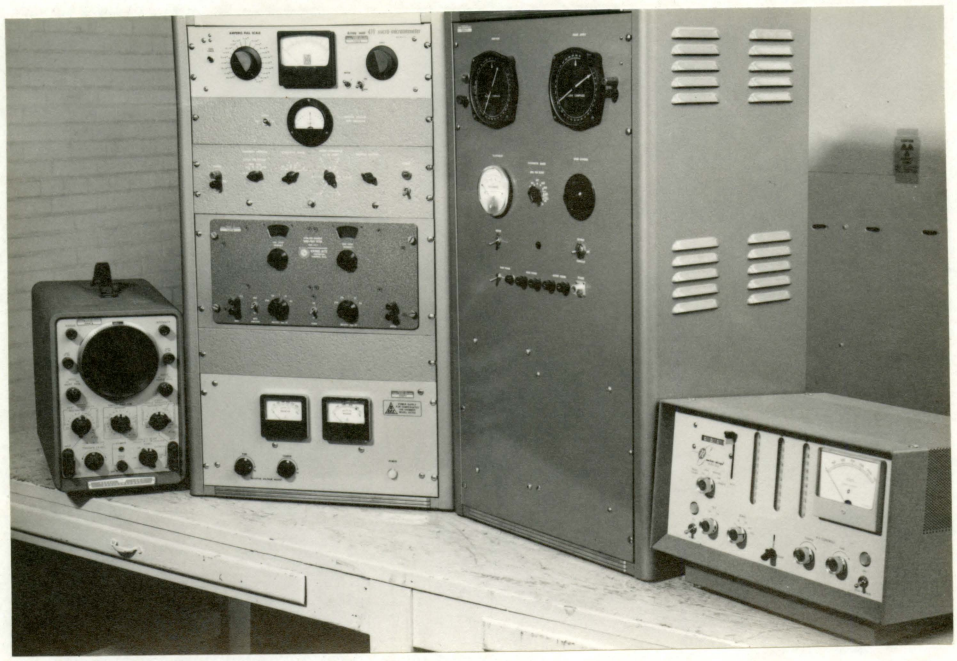

Figure 4. Electronic equipment

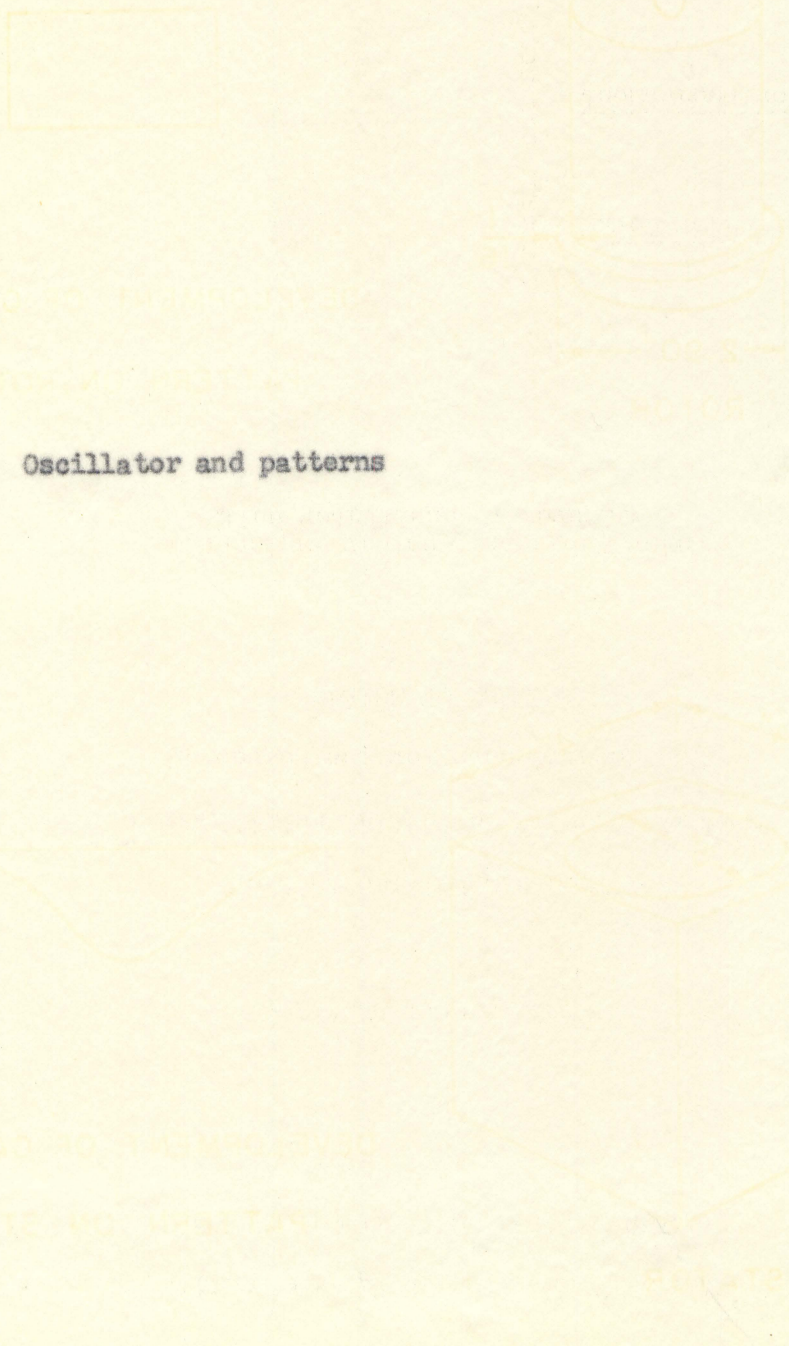

Figure 5. Oscillator and patterns

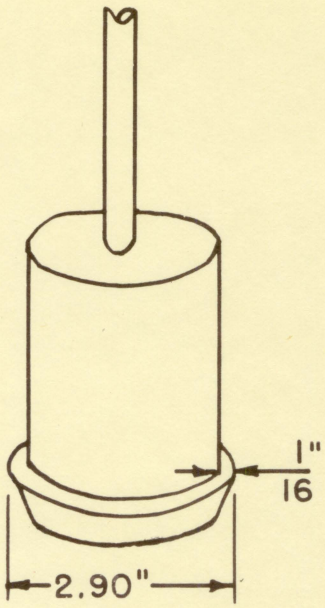

ROTOR

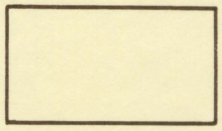

DEVELOPMENT OF CADMIUM PATTERN ON ROTOR

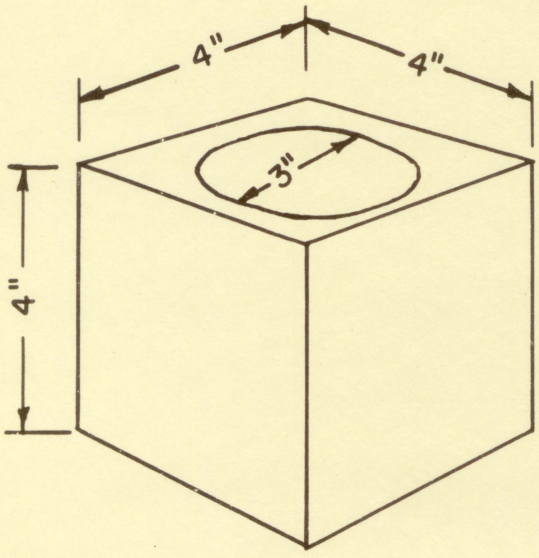

STATOR

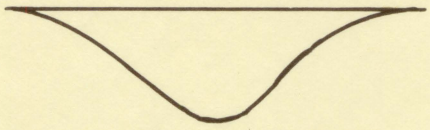

DEVELOPMENT OF CADMIUM PATTERN ON STATOR

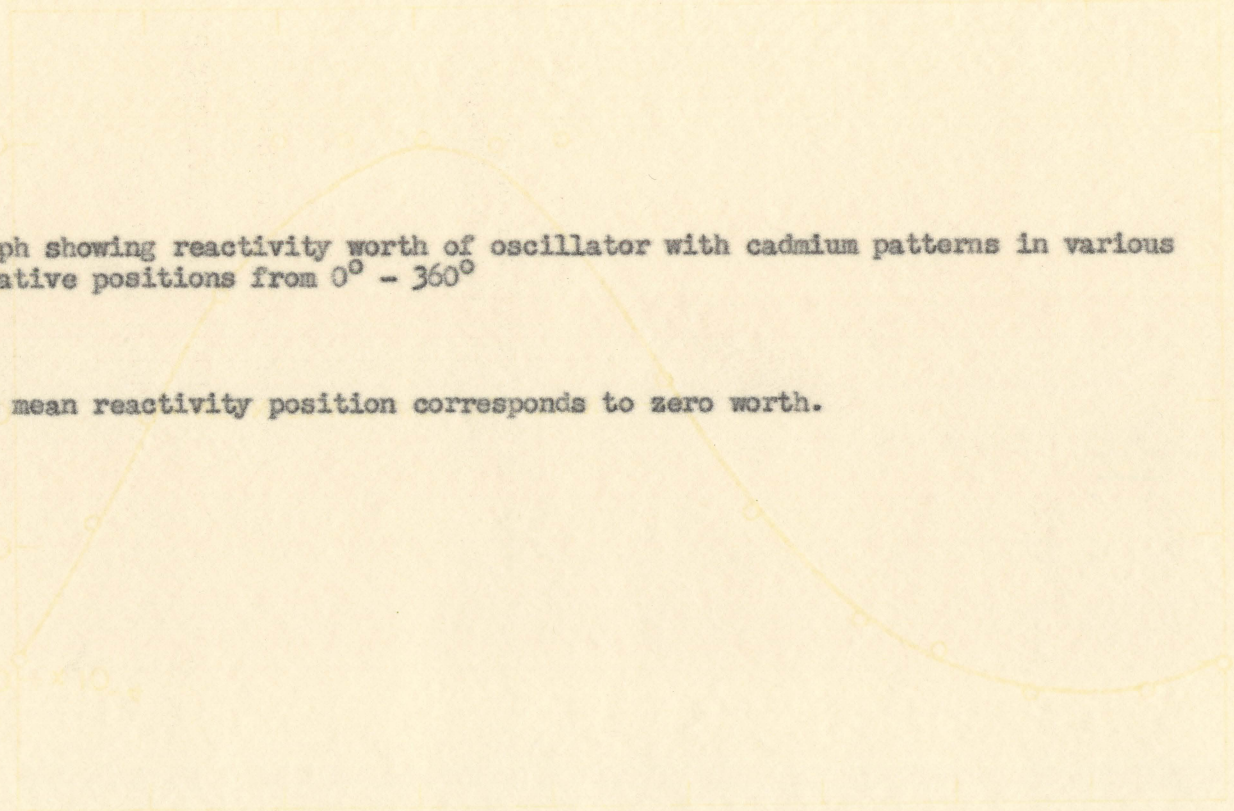

Figure 6. Graph showing reactivity worth of oscillator with cadmium patterns in various relative positions from 0^{o} - 360^{o}

The mean reactivity position corresponds to zero worth.

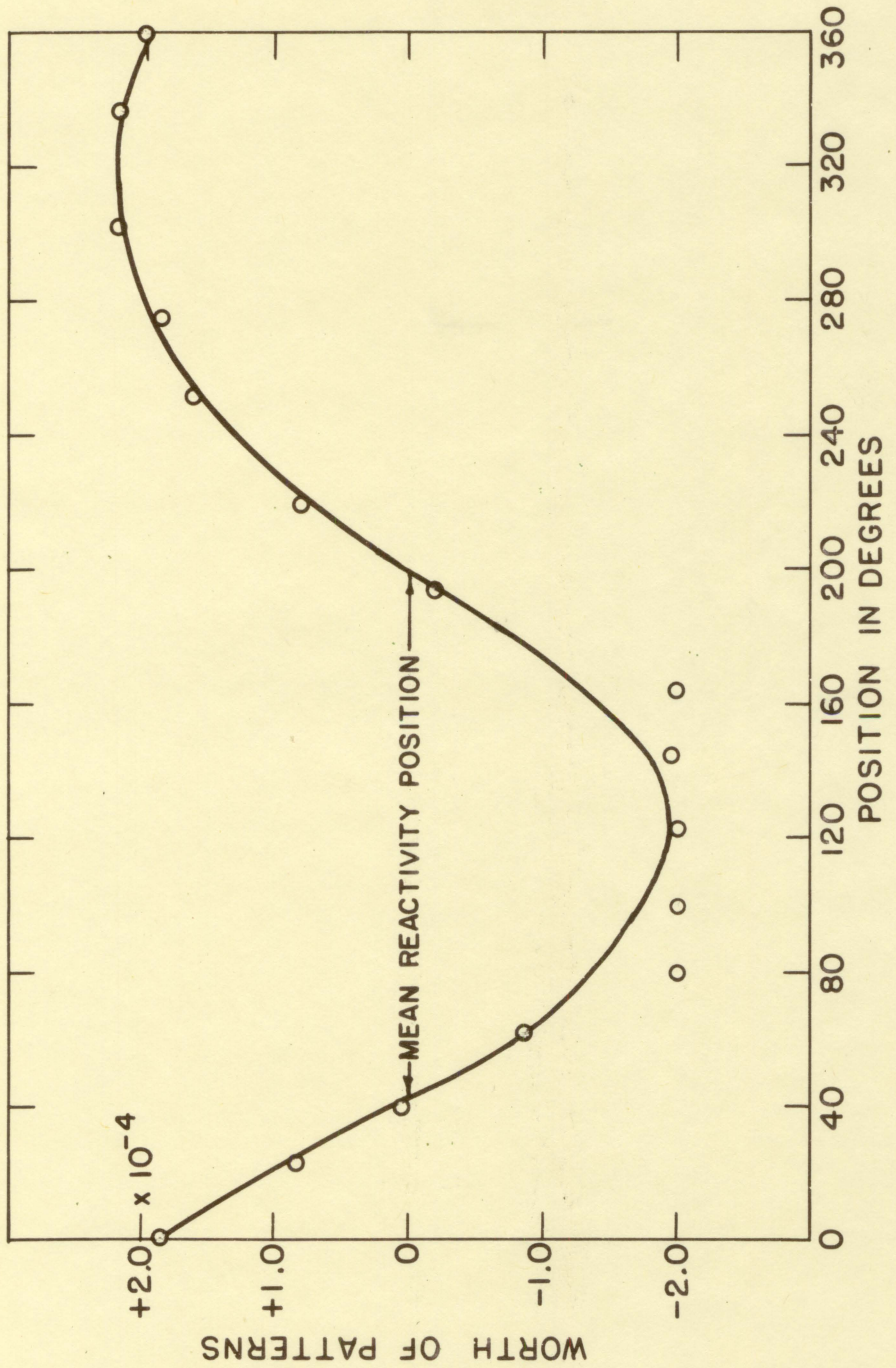
WORTH OF PATTERNS
+2.0
+1.0
0
-1.0
-2.0
x 10^-4
MEAN REACTIVITY POSITION
0
40
80
120
160
200
240
280
320
360
POSITION IN DEGREES

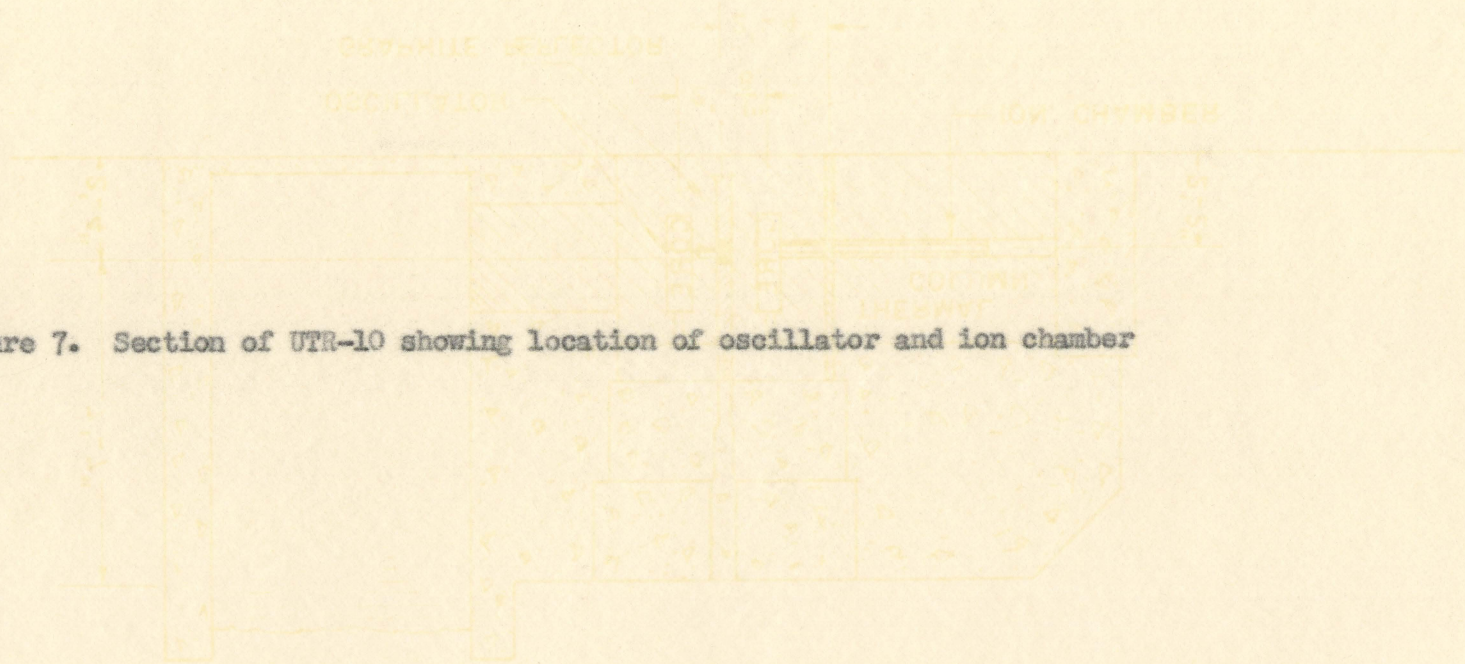

Figure 7. Section of UTR-10 showing location of oscillator and ion chamber

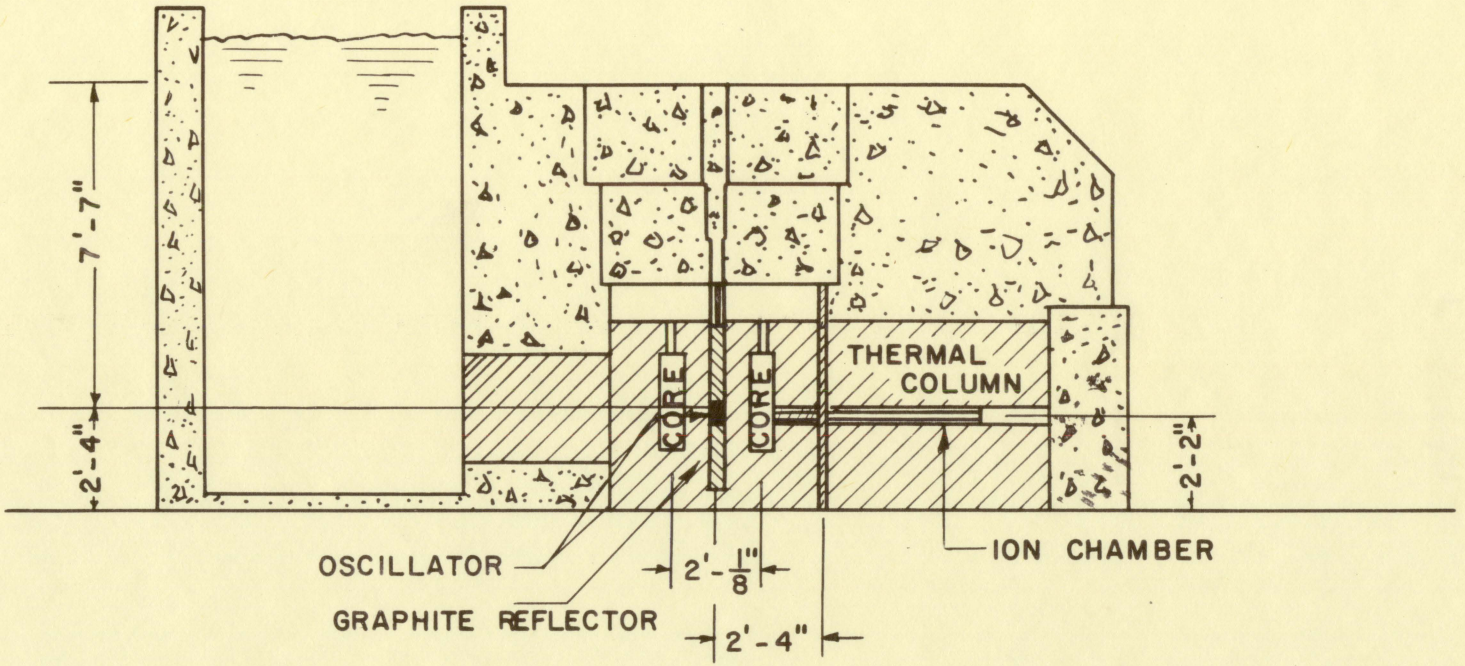
7'-7"
2'-4"
CORE
CORE
THERMAL
COLUMN
2'-2"
OSCILLATOR
GRAPHITE REFLECTOR
2'-1 1/8"
2'-4"
ION CHAMBER

which fed a micro-micro-ammeter. The d.c. output voltage could be bucked out to remove the steady state component, before the output was placed on the oscilloscope screen. The amplitude could be measured directly using the db (decibel) attenuator which allowed adjustment of the pattern to a predetermined size on the oscilloscope. In order to measure the phase angle the output was sent through a band pass filter which selected the frequency of interest to be placed on the screen eliminating harmonics and most noise. The input signal was placed on the scope through a synchro-generator connected directly with the oscillator shaft. The phase of the input could be adjusted through a second synchro-generator which shifted the phase an indicated amount. The resultant Lissajous pattern on the screen could be adjusted until the output and input were precisely in phase. The lag of the output could then be read from the phase adjustment dial. A position synchro-generator attached to the shaft was connected to a scaler which was used to count the revolutions in one minute.

B. Procedure

Since the reactor should be supercritical for approximately half of the cycle and subcritical for the remaining half in order to maintain a steady state, the reactor was made critical in the mean position of reactivity of the patterns. Once this was done all the frequency response data was taken without shutting down the reactor; that is all that could be taken at one time. This was presumed necessary so as not to disturb the flux ratio that was initially established in the two cores. Of course constancy could not be insured since any power drift would have to be corrected by movement of the regulating rod which might change this flux ratio. Once the desired power level was reached the

automatic circuit was put in to maintain a constant level. Then the oscillator was started and adjusted to the proper frequency. To obtain the open loop response the control circuit was then removed from operation.

The runs were conducted at the highest frequencies initially, the speed being slowly reduced to the lowest value possible. This was done because the oscillations were theoretically smallest at the highest frequency and their increase in amplitude could be carefully watched as the frequency was reduced.

In order to read the phase difference directly it was necessary that the pattern input correspond in phase to the synchro-generator output. This was tested by obtaining the phase lag at a frequency of 500 r.p.m. with the motor running both in forward and reverse and noting the difference in the measured phase lag. This was corrected by rotating the stator coils of the synchro-generator to a position halfway between the two previous readings.

A typical oscillation run consisted first of counting the revolutions made by the oscillator in one minute. This was converted to frequency in cycles per second and the band pass filter adjusted to encompass this frequency. Adjustment on the low and high side of this frequency were made equal and each was brought between 2 and 3 percent of the median value given by the scalar. The signals were then brought into phase with the phase dial using the horizontal gain as necessary to give a readable pattern. When this was done the horizontal gain of the scope was brought to a position to be used throughout the experiment. The overall size of the pattern was brought down to 2 cm. on the screen with the db

attenuator. Thus the logarithmic amplitude gain and the phase difference were measured directly. The power level was read at each frequency since the transfer function was directly dependent on the steady-state power level. A simple correction was then applied to the amplitude using the logarithm of the ratio of the two power levels with the power level at the start of the runs as base power level.

The operating power level was ten watts which yielded a chamber current of approximately 2×10^{-7} amperes. The shutdown procedure required that the reactor be "scrammed" before the oscillator was turned off. This prevented the patterns from coming to rest in a position that would add reactivity to the system and cause a positive period.

V. DISCUSSION AND RESULTS

The results of the frequency response tests appear in Figures 8 and 9 and the data in Table 1. The amplitude curve has been normalized to a frequency (ω_N) of 1.0 radians per second, that is $A_{db} = 0$ at 1.0 radians per second. The phase data have been plotted so that the phase lag at the break frequency deduced from the amplitude curve is $-\pi/4$ or -45°. It can be seen that the frequencies investigated correspond primarily to the range influenced by the factor

$$\frac{1}{s + \dfrac{\alpha_o a - \sqrt{\alpha_o^2 a^2 - 4\alpha_o \beta_b}}{2\ell}}$$

in the high frequency analysis of the two core transfer function given previously. This was calculated as $1/(s + 46.8)$ using the parametric values of Danofsky (5). The break frequency derived from the amplitude curve was 33.9 radians per second. The presumption is made first that this break frequency is essentially independent of R, the flux ratio in the two cores. This is particularly true when R is close to 1. R appears in the terms a and b in both cases as $R + 1/R$. As R varies between 1 and 1.2, $R + 1/R$ varies between 2 and 2.03. A mean value then of 2.02 for this term can be assumed so that α_o and ℓ remain the parameters under investigation. Figure 10 shows the variation of ℓ for variously assumed values of α_o with $R + 1/R = 2.02$. To further extend the investigation to include R Figure 11 shows the variation of α_o with ℓ for various values of R from 1 to 3. The extreme values

Figure 8. Experimental curve showing relative output amplitude vs oscillation frequency

Break frequency (asymptotic) = 5.4 cps or 33.9 radians/sec.

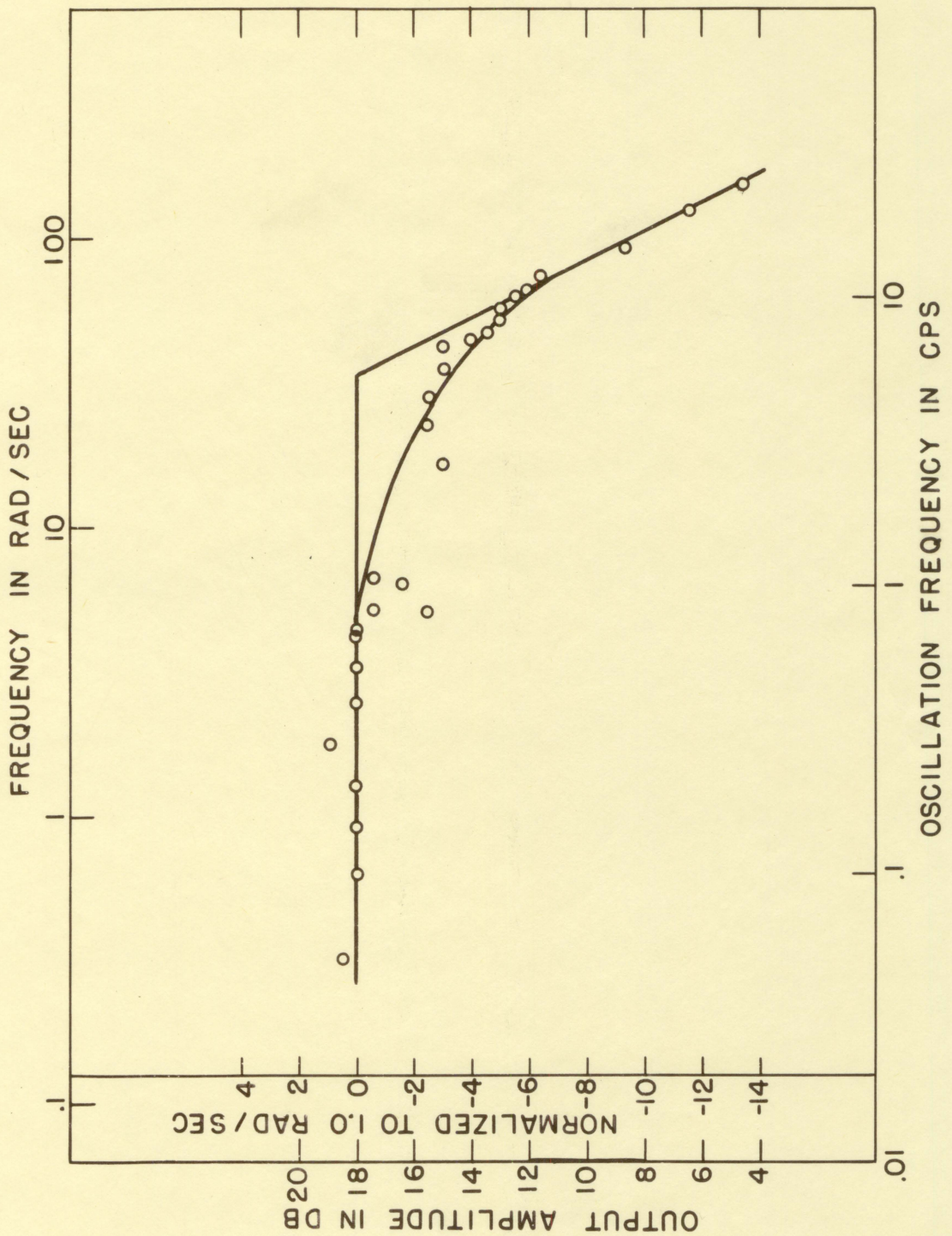
FREQUENCY IN RAD/SEC
.1
1
10
100
OSCILLATION FREQUENCY IN CPS
.01
.1
1
10
OUTPUT AMPLITUDE IN DB
NORMALIZED TO 1.0 RAD/SEC
20
18
16
14
12
10
8
6
4
4
2
0
-2
-4
-6
-8
-10
-12
-14

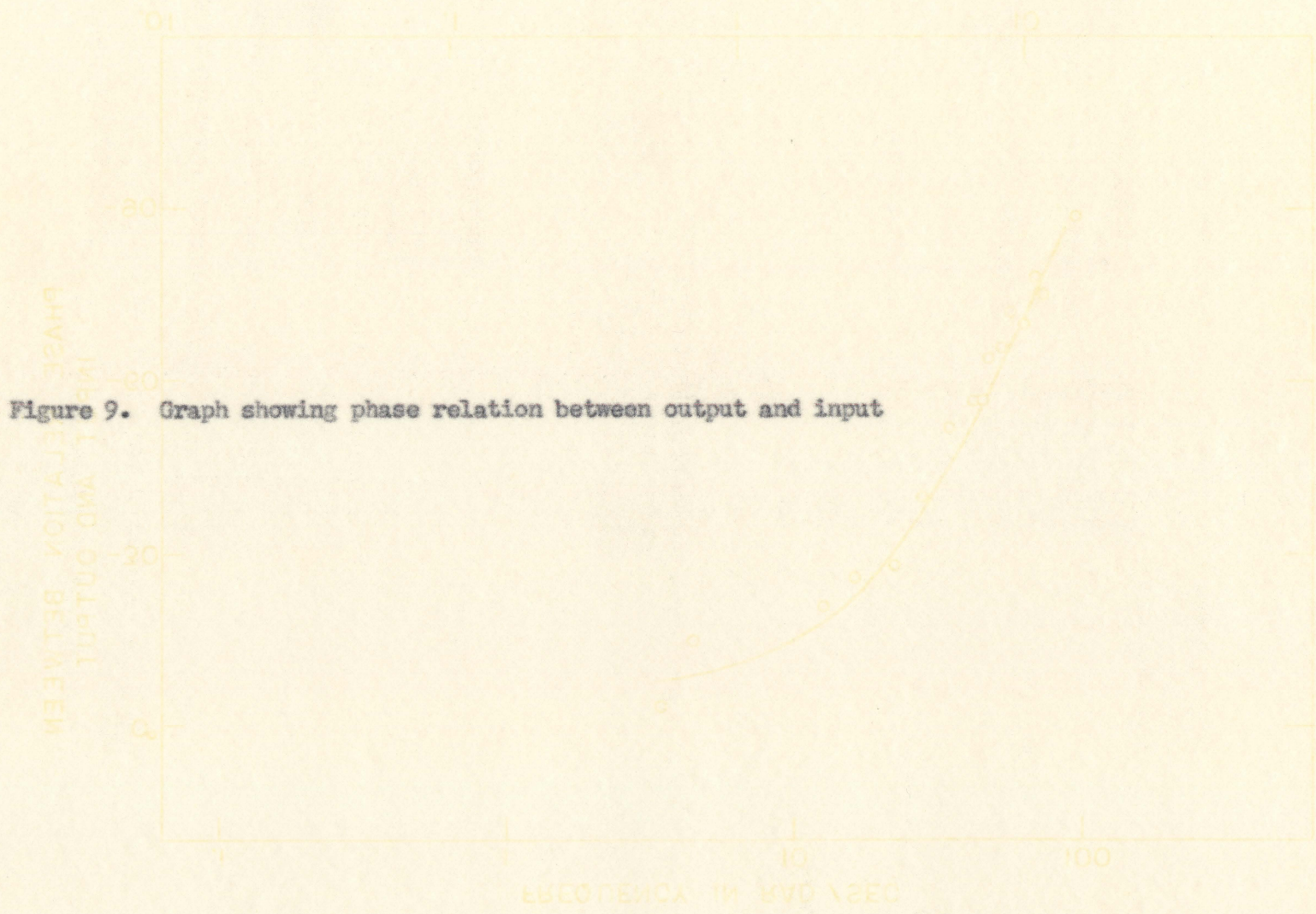

Figure 9. Graph showing phase relation between output and input

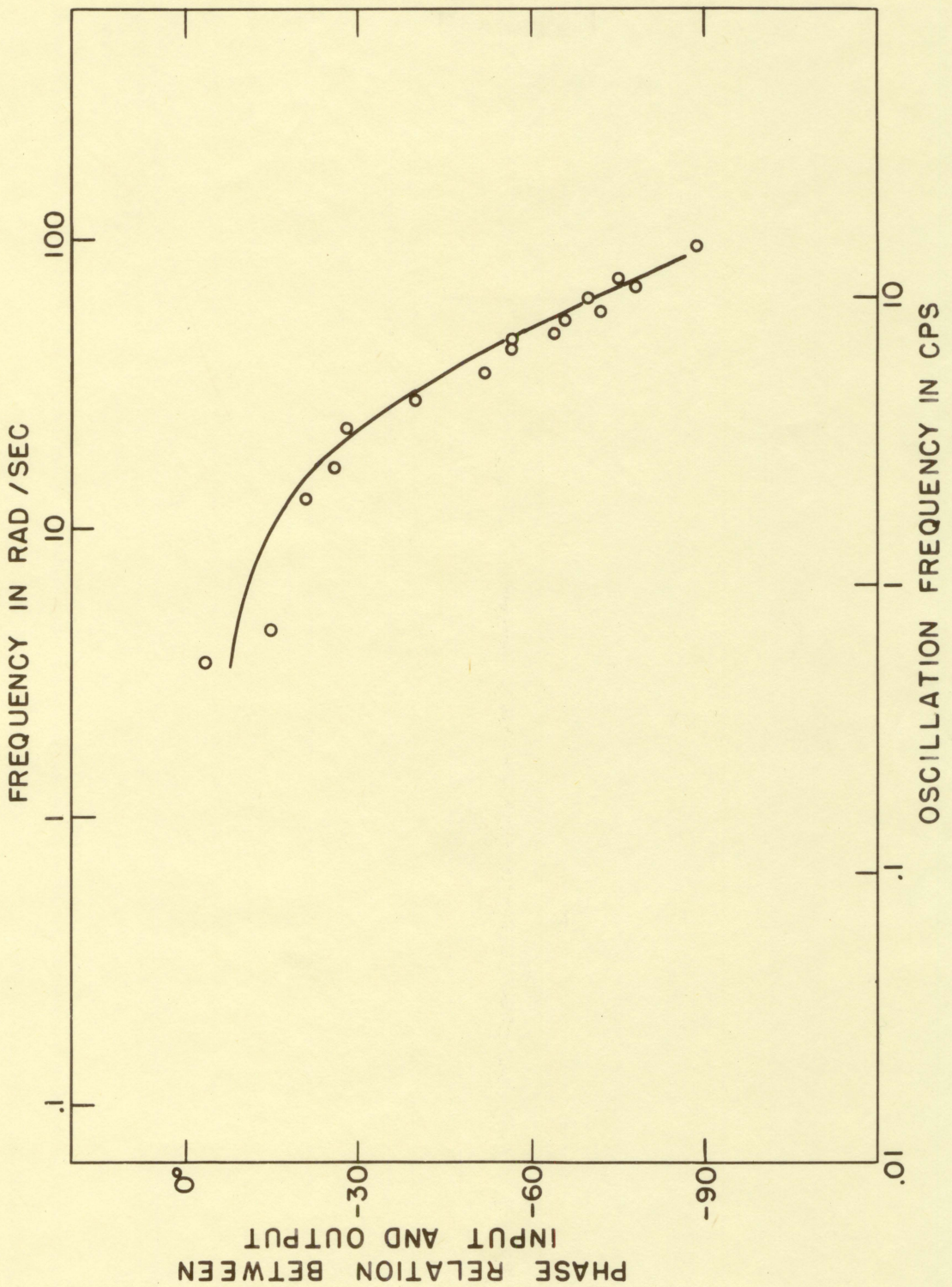
FREQUENCY IN RAD /SEC
100
10
1
.1
PHASE RELATION BETWEEN
INPUT AND OUTPUT
0°
-30
-60
-90
OSCILLATION FREQUENCY IN CPS
10
1
.1
.01

Table 1. Experimental data

Oscillator tachometer	Speed(RPM) counter	Frequency CPS	Band pass range Low	Band pass range High	Power ion chamber amp.	DB atten.	Phase dial
3	3.1	.051	.0495	.0520	.192	18.5	—
6	5.9	.099	.095	.103	.192	18.0	—
9	8.6	.145	.140	.150	.192	18.0	—
12	11.8	.197	.194	.200	.192	18.0	—
18	16.8	.280	.275	.285	.190	19.0	—
24	23	.389	.380	.400	.192	18.0	—
30	31	.518	.500	.530	.190	18.0	265
40	39	.665	.650	.680	.190	18.0	—
40	42	.700	.680	.720	.185	18.0	277
50	48	.800	.780	.820	.190	15.5	—
50	50	.833	.820	.845	.190	17.5	—
60	60	1.00	.980	1.020	.185	16.5	—
60	61	1.018	.990	1.030	.190	17.5	—
120	121	2.00	1.95	2.050	.190	—	283

Table 1. (Continued)

Oscillator tachometer	Speed (RPM) counter	Frequency CPS	Band pass range		Power ion chamber amp.	DB atten.	Phase dial
			Low	High			
160	156	2.60	2.50	2.70	.190	15.0	288
210	211	3.50	3.40	3.60	.195	15.5	290
270	264	4.40	4.20	4.60	.192	15.5	302
345	333	5.55	5.30	5.80	.192	15.0	314
420	400	6.67	6.30	7.00	.190	15.0	319
445	425	7.1	6.90	7.30	.190	14.0	319
470	450	7.5	7.25	7.75	.187	13.5	326
525	496	8.3	8.00	8.60	.185	13.0	328
565	533	8.9	8.50	9.30	.190	13.0	334
625	593	9.9	9.50	10.30	.190	12.5	332
675	645	10.7	10.50	11.0	.195	12.0	340
730	694	11.6	11.3	11.9	.195	11.5	337
930	898	15.0	14.75	15.25	.195	8.5	351
1200	1175	19.6	19.2	20.0	.185	6.5	---
1510	1461	24.3	24.0	24.6	.185	4.5	---

Figure 10. Graph showing variation of ℓ with α_o for $R + \frac{1}{R} = 2.02$ (see discussion)

$$\omega_{\text{Break}} = \frac{\alpha_o a - \sqrt{\alpha_o^2 a^2 - 4\alpha_o \beta_b}}{2\ell}$$

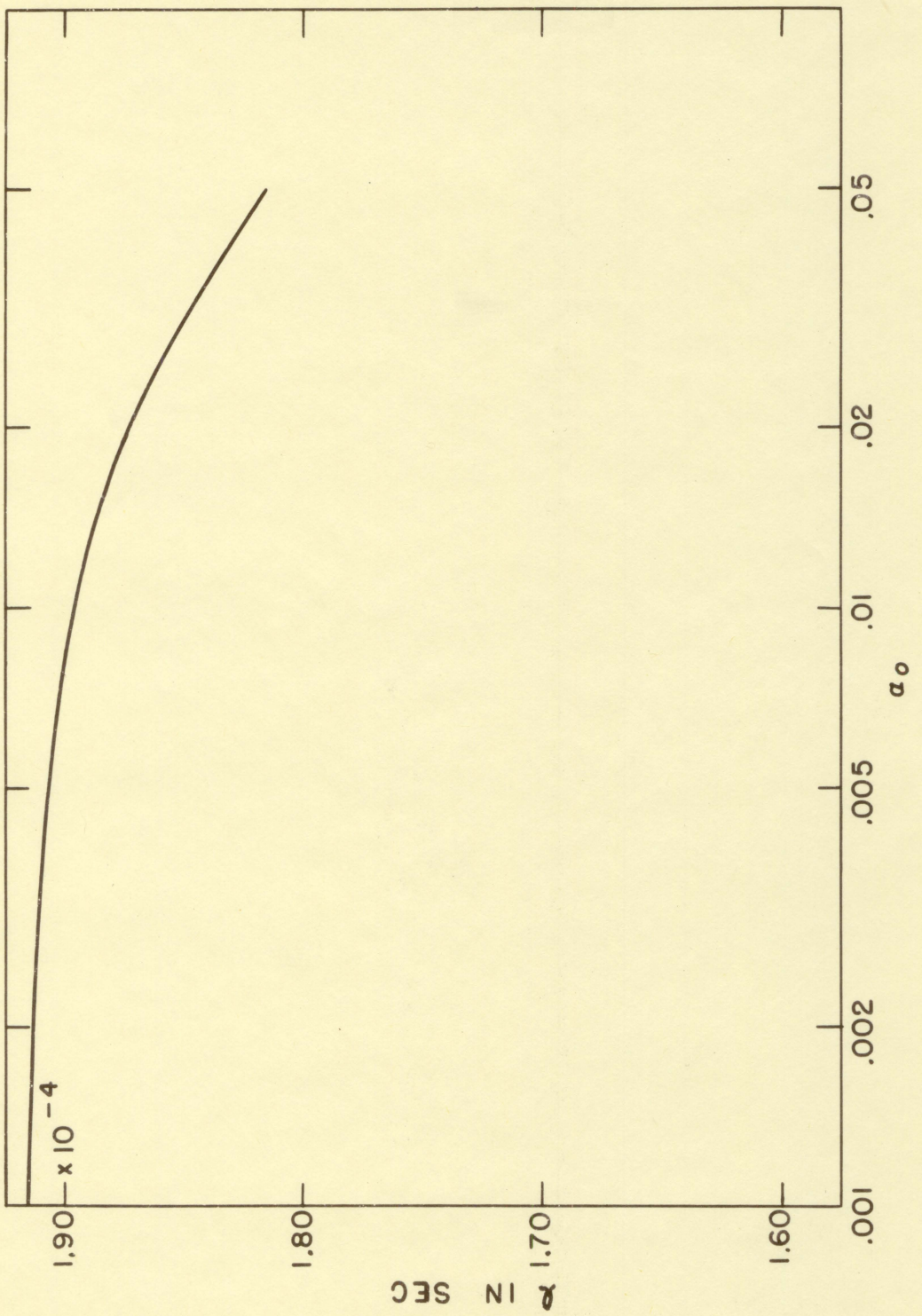
1.90
1.80
1.70
1.60
× 10⁻⁴
γ IN SEC
.001
.002
.005
.01
.02
.05
a_o

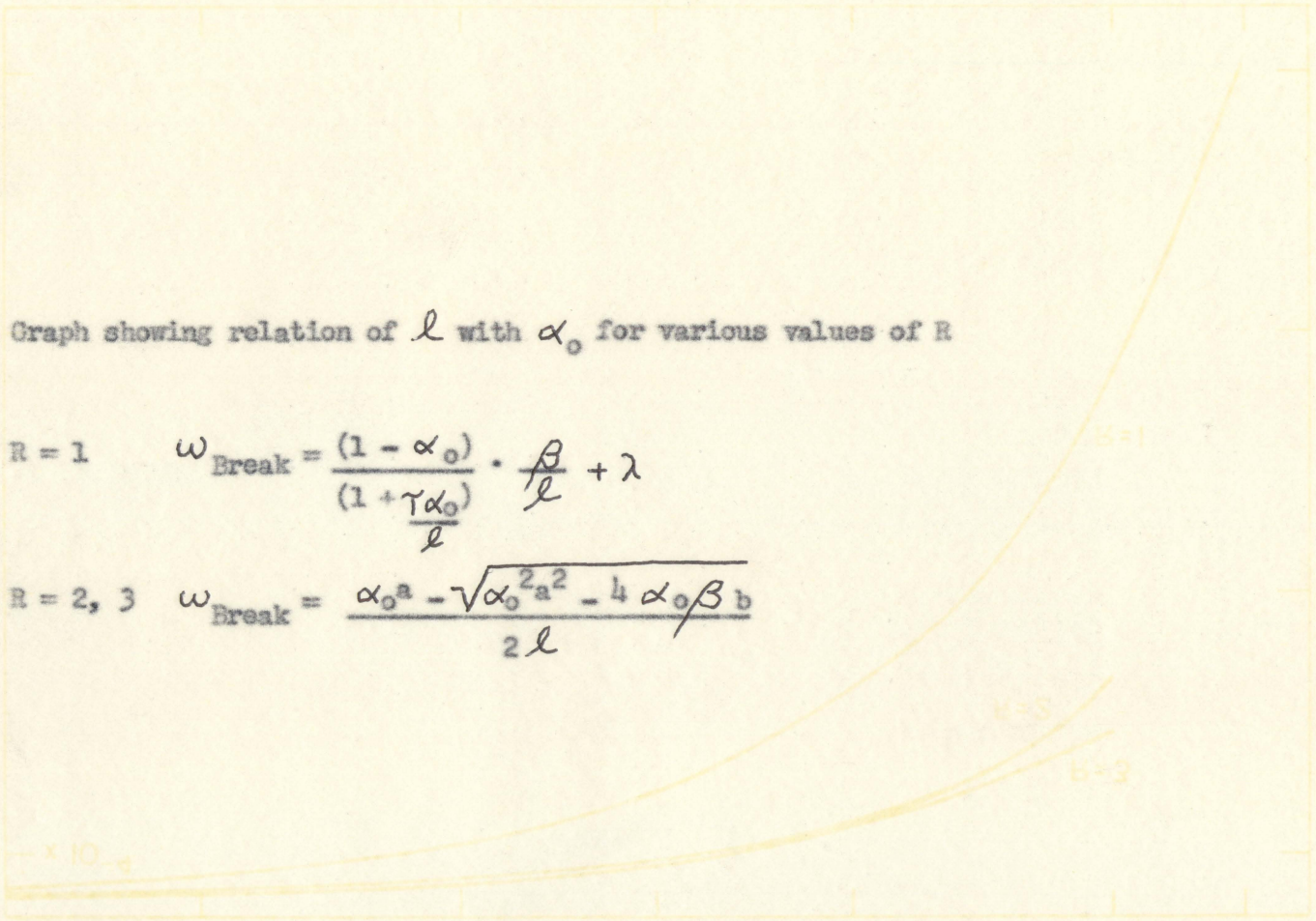

Figure 11. Graph showing relation of ℓ with α_o for various values of R

$$R = 1 \qquad \omega_{Break} = \frac{(1 - \alpha_o)}{(1 + \frac{\tau \alpha_o}{\ell})} \cdot \frac{\beta}{\ell} + \lambda$$

$$R = 2, 3 \qquad \omega_{Break} = \frac{\alpha_o a - \sqrt{\alpha_o^2 a^2 - 4 \alpha_o \beta b}}{2\ell}$$

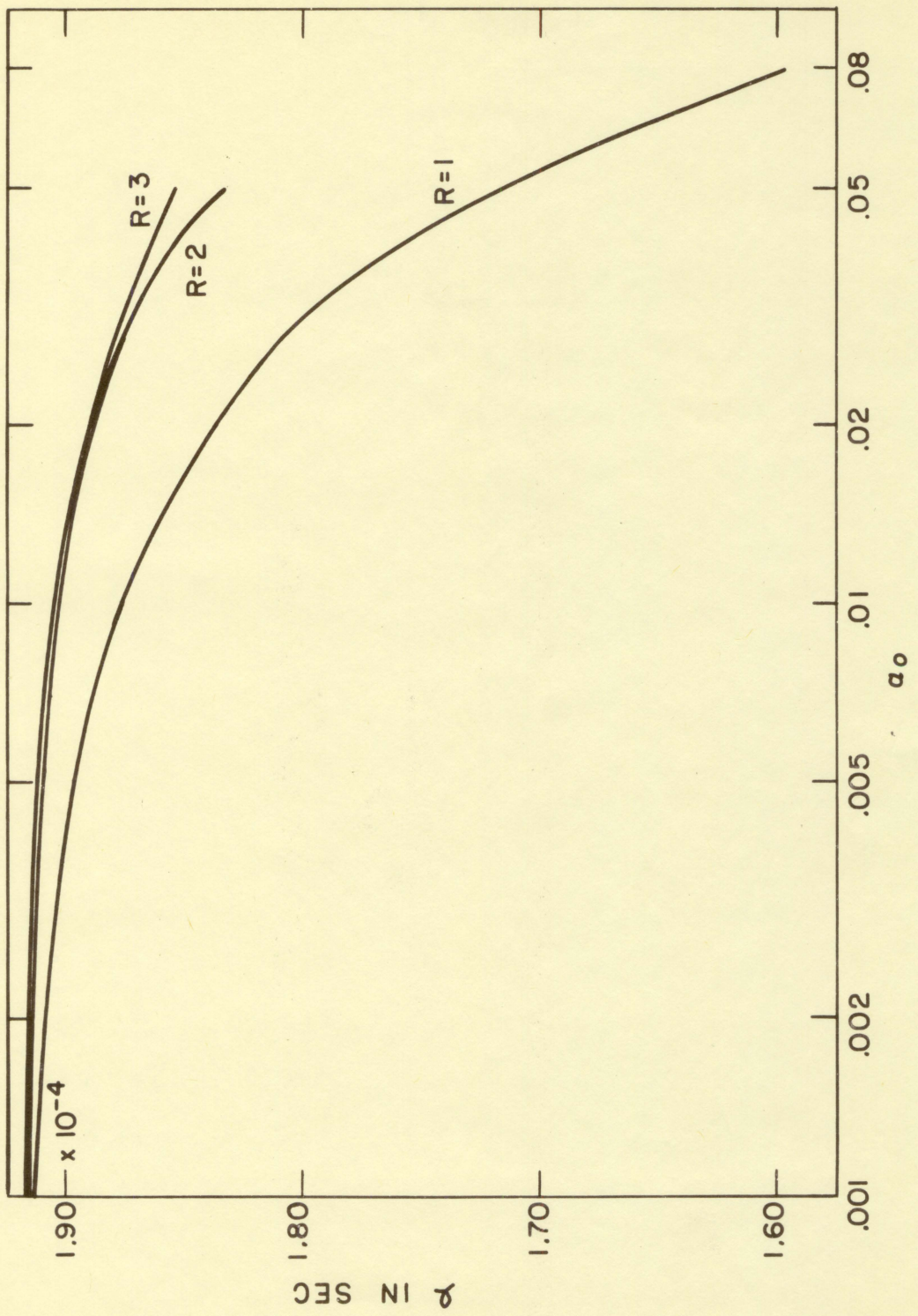
R=3
R=2
R=1
x 10⁻⁴
1.90
1.80
1.70
1.60
γ IN SEC
.001
.002
.005
.01
.02
.05
.08
a₀

of R would probably not be encountered in normal operation of the two core system, but Baldwin (3) states that foil activations have shown the flux ratio to vary from 1 to over 2 on various occasions in the Argonaut.

From Figure 10 it was noted that ℓ does approach the asymptote of β/ω break of 1.917×10^{-4} seconds as α_o approaches zero. The behavior of the function with increasing α_o also may have been expected. As can be seen the value of ℓ decreases with increasing α_o. The mean prompt thermal neutron lifetime for a finite reactor was defined as $\mathcal{L}_t / v \Sigma_a$ where $\mathcal{L}_t$ is the thermal non-leakage probability. If the coupling increases as evidenced by increasing α_o then more neutrons must be leaking from the cores, hence $\mathcal{L}_t$ would decrease. The decrease in ℓ is then obvious. With α_o equal to 0.0155 as given by Danofsky (5) the value of ℓ is 1.884×10^{-4} sec.

Figure 11 shows that as R increases ℓ deviates less from its asymptotic value for a given α_o. Probably the increasing dominance of one core over the other in the production of neutrons produces behavior that more closely approximates that of a single core.

The curve for R = 1 was drawn using the simplified transfer function for this special case as derived in Chapter II. While it is more accurate than the curves drawn from the high frequency analysis it is applicable only for this special case which probably did not obtain during the course of the experiment.

The final value of ℓ was determined from Figure 10 at α_o equal to 0.0155. The upper and lower limits to this value of 1.884×10^{-4} sec. were set as follows:

(1) Assume the value of α_o not more than 0.030 nor less than

0.005.

(2) Assume R no greater than 2 while 1 serves as the lower limit. The upper limit of α_o was set arbitrarily and was presumed a reasonable value for the UTR-10. The lower limit was set by considering the fact that the equipment when immersed in the internal reflector had a total worth of 0.0030. Since it is the coupling that is primarily affected in this position there must be at least this fraction of total neutrons interchanged between the cores. The limit was chosen somewhat higher since evidently some residual coupling effect must exist for the reactor to be made critical. While values of R less than 1 may be encountered they need not be considered since R always appears as R + 1/R in the break frequency analysis.

Within these limits then the value of ℓ may vary from 1.805×10^{-4} sec. at R = 1 and $\alpha_o = 0.030$ to 1.910×10^{-4} sec. at R = 2 and $\alpha_o = 0.005$.

A prime consideration in the performance of the experiment was that the rotor turn evenly in two respects. The first was that within each revolution the angular velocity be constant. This was necessary so that rotation produce the sinusoidal variation in reactivity as shown by the calibration curve (Figure 6). Any further distortion due to irregularity of rotation could produce undesirable harmonics. The second consideration was that the rotor maintain a constant speed throughout a run. This was essential to minimize errors in reading. Significant changes in rotor speed would displace the patterns on the oscilloscope screen changing both amplitude and phase data.

For these reasons strict alignment of bearings was required. To

overcome imperfect alignment it was necessary to place two flexible hard-rubber couplings along the shaft. Thus the mechanical problem was solved and possible random fluctuations in phase readings was considered a minor objection to the use of this type of flexible coupling (10b).

It was presumed that the ion chamber did not introduce significant phase errors at the frequencies investigated. However, the bandwidth of the band pass filter did appear to have a significant effect on both the frequency and phase readings. This was due probably to the combined effect of harmonics and noise. It was found however that if the bandwidth was kept within 2 or 3% of the median frequency and adjusted to enclose an equal range on each side of this frequency that there was little distortion of the wave pattern on the oscilloscope. Larger and uneven widths seemed to shift the phase and as the bandwidth was increased the output amplitude showed a corresponding increase.

It was found that at high frequencies (above 6 cps) the phase and amplitude measurements were made easily using the Lissajous patterns on the oscilloscope screen. At lower frequencies however, readings became increasingly difficult. This was attributable to the low persistence of the oscilloscope screen. At these lower frequencies the left side of the pattern would disappear before the beam had swept back to reinforce the image.

A second method therefore of determining the phase of the output at low frequency (1 cps and less) consisted in the superposition of output and input on a dual trace scope. Adjustment of the input phase again gave the phase lag when the patterns coincided.

It was found that the db attenuator reading in steps of .5 decibels

was quite sufficient and that finer steps would not have produced greater accuracy in conjunction with the method used to read the decibel gain.

Other improvements suggested for the equipment aside from a more precise alignment of bearings were

1. Either immersion of the bevel gears in oil to reduce wear and noise or replacement by a worm gear drive.

2. Placement of two more bearings to keep shaft and oscillator from "whipping."

3. Replacement of bronze bearings with roller or ball bearings.

4. Further reduction of the pattern size to lower the static worth of the equipment. This would serve the dual purpose of making the experiment safer and preventing the reactor from being "sluggish."

VI. SUGGESTIONS FOR FURTHER WORK

The experimental work showed that investigation of the transfer function of a two-core reactor system is possible by measurement of the frequency response to sinusoidal oscillation of the coupling. The break frequency was distinct and easily analyzed. However, as was demonstrated there are a number of factors which all contribute to the value of the break frequency that was investigated. Many of these factors were not known precisely while even the order of magnitude of others was not definite. This latter case refers to τ while in the former reference is made to β, R, α_o, ℓ and λ. In this study the prime objective was to determine ℓ and the break investigated could be approximated by β/ℓ or a more complicated function involving most of the above terms. In any event the precise determination of ℓ was based on only assumed values of the other parameters. In this light further work, it is suggested, should be extended to other frequencies encompassing all theoretically derived break frequencies that is from 0.06 radians per second to 400 radians per second.

If these other breaks, of which there are five more, are visible and measurable then since each is derivable in terms of the above six parameters it should be possible to determine all of them fairly precisely without recourse to assumptions.

Lower frequencies could be easily obtained by simply coupling another 30 to one gear reducer to the motor along with the present one. However, higher frequencies using the motor available would only be possible by introducing five or six full sinusoidal patterns per

revolution of the oscillator.

It is further suggested that the transfer function be investigated with the ion chamber in various positions to detect the reactor response. The reactor may behave more as a single core reactor in the position it was for this experiment that is in the thermal column than it would had it been located between the cores.

Finally an attempt may be made to detect the transfer function of each core separately. As a result of any flux tilting that may be present the transfer function of each core would be different. An ion chamber located at each core to detect its output and preferably shielded from neutrons arriving directly from the other core may yield significant results about the magnitude and variation of flux tilting.

VII. CONCLUSIONS

The frequency response analysis of a two-core system utilizing a centrally located varying absorber was shown to be feasible. The results manifested in the transfer function show a clearly defined break at approximately the theoretically derived frequency.

Understanding of the two-core transfer function as derived by Baldwin (3) has been made clearer by analyzing separately the high and low frequency response. While the original purpose of this investigation was to discover the break frequency corresponding to β/ℓ of the single core transfer function, so that finally ℓ may be determined, it is concluded that the other parameters beside β need be known more precisely than they are at present for the final evaluation of ℓ. Of course assigning limits within which the UTR-10 can be assumed to behave can in combination with the experimentally determined value of the break frequency yield useful information as to the expected range that may be assigned ℓ. Hence it was concluded that the value of ℓ was equal to 1.884×10^{-4} sec. and was no greater than 1.805×10^{-4} sec. and no less than 1.910×10^{-4} sec. Here it is insufficient knowledge of the values of the other parameters rather than experimental error that imparts such uncertainty to this value. To establish the range for ℓ the precise knowledge of β and τ was assumed while α_o and R were allowed to fluctuate between reasonable limits for the UTR-10 as discussed in Chapter 5.

The UTR-10 response was similar to what would be expected of a single core response, but as a result of coupling there are other break

frequencies that occur in limited ranges affecting the transfer function slightly and only in these ranges. The reactor response naturally deviates further and further from single core response the more significant the effect of coupling.

The transfer function derived by Baldwin (3) was valid for the UTR-10 behavior at least in the range of frequencies investigated, that is from 0.32 radians per second to 157 radians per second. To absolutely validate his transfer function for the UTR-10 it is necessary to know all the parameters accurately so that precise locations of the break frequencies are known. Rather than this approach, since determining the parameters by direct measurement would be difficult, it was suggested that the transfer function high and low frequency analysis be assumed applicable to the UTR-10 so that further investigation of the transfer function to higher and lower frequencies would yield fairly accurate values of the parameters.

In conclusion if further work is carried out it is suggested that the low frequency response, less than 10 radians per second, be measured on a recorder rather than an oscilloscope. The low frequency patterns become indistinguishable and permanent recording of the response is advised.

The experiment proved safe and the reactor showed veritably no power drift during the course of the oscillation runs. A level of 10 watts was used rather than the originally proposed level of 1 watt in order to give larger more easily analyzable oscillation amplitudes.

VIII. SUMMARY

The transfer function of the two core UTR-10 reactor was investigated by frequency response analysis using a centrally located varying absorber. The range of frequency of oscillation used was 0.32 radians per second to 157 radians per second. The experimental value of the break frequency was 33.9 radians per second. The prompt thermal neutron lifetime, ℓ, was 1.884×10^{-4} sec. and had limits of 1.805×10^{-4} sec. and 1.910×10^{-4} sec. for α_o between .005 and 0.030 and R between 1 and 2 with the remaining parametric values those assumed by Danofsky (5).

The experiment showed that the technique was feasible and produced clearly defined results. The need for precise values of the parameters was noted and the possibility of determining them through the extension of the frequencies investigated was suggested.

An analysis of the separate high and low frequency response yielded the following break frequency in the range investigated:

$$\omega_{break} = \frac{\alpha_o a - \sqrt{\alpha_o^2 a^2 - 4 \alpha_o \beta b}}{2\ell} .$$

These quantities are defined in the nomenclature. The limiting frequency when α_o approaches zero is β/ℓ which corresponds to the single core break frequency.

Suggested improvements on the technique used included reduction of pattern size and the use of a recorder for data at frequencies less than 10 radians per second.

IX. NOMENCLATURE

a - $R + 1/R + 2\beta/\alpha_o + 2\alpha_o\tau/\ell$

A_{db} - amplitude of oscillation, decibels = $20 \log A\omega / A\omega_N$

b - $R + 1/R + \beta/\alpha_o$

B^2 - Buckling, $cm.^{-2}$

C_i - i th delayed neutron precursor concentration, $atoms/cm.^3$

δC_i - small change in the i th delayed neutron precursor concentration, $atoms/cm.^3$

D - thermal diffusion coefficient, cm.

k - multiplication constant in an infinite medium, dimensionless

k_{eff} effective multiplication constant for a finite reactor, dimensionless

k^{ex} - multiplication constant in excess of 1, defined as $k_{eff} - 1$, dimensionless

δk - in single core reactor - excess multiplication factor defined as $(k_{eff} - 1)/k_{eff}$, dimensionless

ℓ - in two core reactor, - mean prompt neutron lifetime in core and associated reflector, seconds

ℓ_o - mean prompt thermal neutron lifetime in infinite homogenous reactor, seconds

ℓ^* - mean prompt thermal neutron lifetime for single core infinite reactor, seconds

$\mathcal{L}$ - in single core reactor, - neutrons escaping from the reactor/neutrons absorbed in the reactor, dimensionless
in two core reactor,-probability of neutron escaping from individual core while slowing down, dimensionless

L - thermal diffusion length, cm.

n - neutron population, $neutrons/cm.^3$

δn - small change in neutron population from previous steady state population, $neutrons/cm.^3$

p - resonance escape probability, dimensionless

R - flux ratio in the two cores of a two-core reactor, n_1^o/n_2^o, dimensionless

s - Laplacian operator, $sec.^{-1}$

S - total source of thermal neutrons, neutrons/sec. cm^3

S_d - source of thermal neutrons as a result of the decay of neutron precursors, neutrons/sec. $cm.^3$

S_p - source of thermal neutrons as a result of the prompt emission of fast neutrons on fission, neutrons/cm^3 sec.

S_{12} - source of thermal neutrons in first core arising from second core as a result of passage through the internal graphite reflector, neutrons/cm^3 sec.

$T.F._1$ transfer function of first core, $\delta n_1 / \delta \alpha_o n_1^o$, dimensionless

v - mean velocity of thermal neutrons, cm./sec.

α - coupling coefficient, dimensionless

$\delta\alpha$ - small change in coupling coefficient from previous steady state condition, dimensionless

β - total fraction of fission products that are delayed neutron precursors, dimensionless

β_i - fraction of fission neutrons that arise from the i th delayed neutron precursor, $_i$ = , dimensionless

$$\nabla^2 \quad \frac{\partial^2}{\partial x^2} + \frac{\partial^2}{\partial y^2} + \frac{\partial^2}{\partial z^2}$$

ϵ - proportionality constant between the flux in one core at a time $(t - \tau)$ and the source of thermal neutrons arriving at the other core from this source at time t

λ - decay constant averaged over all the delayed neutron groups taking into account the abundance of each of the i groups, $cm.^{-1}$

λ_i - decay constant of the i th group of delayed neutron precursors, $cm.^{-1}$

ν - neutrons released per fission

Σ_a - total absorption cross section of core material, $cm.^2$

τ - the time it takes neutrons arising in one core to appear as a source of thermal neutrons in the other core

ϕ - neutron flux (thermal), neutrons/$cm.^2$ sec.

ω - oscillation frequency, radians per second

ω_N - base frequency whose amplitude is normalized to 1, $A_{db}\omega_N = 0$, radians/sec.

ω_{Break} - break frequency

Subscripts and superscripts

0 - steady state value of parameter

1 - parametric value in core 1

2 - parametric value in core 2

X. BIBLIOGRAPHY

1. Akcasu, Z. General solution of the reactor kinetic equations without feedback. Nuclear Science and Engineering 3: 456-467, 1958.

2. Avery, R. Theory of coupled reactors. 2nd United Nations International Conference on the Peaceful Uses of Atomic Energy, 1958. Proceedings 12: 182-191, 1958.

3. Baldwin, G. C. Kinetics of a reactor composed of two loosely coupled cores. Nuclear Science and Engineering 6: 320-327, 1959.

4. Cordy, R. N. Kinetics experiments on water boilers - "A" core report. Part 3 - Pile oscillator results. United States Atomic Energy Commission Report NAA-SR-5417, North American Aviation., Downey, Calif.

5. Danofsky, Richard A. Kinetic behavior of coupled reactor cores. Unpublished M.S. Thesis. Ames, Iowa, Library, Iowa State University of Science and Technology, 1960.

6. Franz, Joseph P. Pile transfer functions. United States Atomic Energy Commission Report AECD-3260, Technical Information Service Extension, AEC . 1949.

7. Glasstone, S. and Edlund, M. C. The elements of nuclear reactor theory. Princeton, N. J., D. van Nostrand Company, Inc., 1952.

8. Harrer, R. E., Boyar, R. E. and Krucoff, D. Transfer function of Argonne CP-2 reactor. Nucleonics 10, No. 8: 32-36, August 1952.

9. Hill, J. F. Reactor Physics 12, Nuclear Power 2: 201-205, 1957.

10a. Keppin, G. R. and Wimett, T. F. Reactor kinetic functions: a new evaluation. Nucleonics 16, No. 10: 86-90, Oct., 1958.

10b. Lundholm, J. G., Griffin, C. W. and Meise, E. R. Measurement of zero power frequency response of the SRE. United States Atomic Energy Commission Report NAA-SR-3762, North American Aviation., Downey, Calif. 1960.

11. Nordheim, L. W. Pile kinetics. United States Atomic Energy Commission Report MDDC-35, Manhattan District, Oak Ridge, Tenn. [1946].

12. Shultz, M. A. Control of nuclear reactors and power plants. New York, N. Y., McGraw-Hill Book Company Inc., 1955.

13. St. John, D. S. Reactor stability. United States Atomic Energy Commission Report DP-517, DuPont de Nemours (E.I.) & Co., Wilmington, Del. 1960.

14. University training reactor. American Standard Company. Technical Bulletin No. 106, [1959].

XI. ACKNOWLEDGMENTS

The author wishes to acknowledge the infinite patience and helpful guidance of his major professor, Dr. Glenn Murphy.

The invaluable assistance of Mr. Richard Danofsky deserves mention. His experience and knowledge in the field of reactor kinetics proved of great value to the author both in problems that he did encounter and in problems that he would have encountered were they not pointed out to him in advance.

Thanks are also due to Mr. Ray Prior for his painstaking care in the development of the electronic instrumentation.

Dr. R. E. Uhrig who started the author on this project and who planned the experiment and designed much of the equipment, but who left the university before their completion deserves sincere appreciation from the author.